1. SPECIFIC AIMS

The specific aims (SA) of our multi-institutional BRP Grant can be summarized as follows:

SA 1. Qualitatively and quantitatively assess TCPC flow dynamics for different anatomic geometries and physiologic conditions (rest vs. exercise) in order to establish optimal TCPC templates – *in vitro* experiments, computational fluid dynamics (CFD), *in vivo* animal studies and patient MRI studies.

SA 2. Study the impact of different materials, used in the IVC to RPA connection (in the TCPC surgery), on the local flow dynamics - CFD and *in vivo* animal studies.

SA 3. Establish an anatomic and materials database that would be used to validate computationally based designs and surgical planning - CFD, patient MRI, and animal studies.

SA 4. Provide improved designs and surgical planning through the use of pre-surgery MRI anatomic information and computational simulations, to optimize the TCPC in an individual patient- patient MRI and computer modeling in conjunction with anatomic templates derived from SA 1.

SA 5. Define the effects of flow dynamics of the aorta on the energetics of the Fontan connection- *in vitro* experiments and patient MRI studies.

In order to accomplish the above SAs and improve our understanding of the anatomy and physiology of the Fontan TCPC, we had to devote significant efforts to developing new methods and tools for 3D anatomic and velocity reconstructions based on patient MRI scans. Furthermore, the complexity of the Fontan patient anatomies and the resulting flow fields that we encountered required the development of more robust computational and experimental fluid dynamic techniques for quantitatively evaluating the Fontan connection. The complexity of the geometry is quite enlightening when you review the database of 230 Fontan patient MRI scans gathered during this BRP. The significant technological contributions of this BRP will not only help in the evaluation and surgical planning of the Fontan circulation, but will also provide an innovative and systematic approach for analyzing and "correcting" other cardiovascular flow related abnormalities. Animal studies proved to be quite challenging, as hurdles were faced to model the single ventricle circulation in lambs and keeping them alive after performing the Fontan operation. A summary of the major accomplishments for each SA over the past seven years (7/01/02 – 6/30/09) is provided below:

Fontan databases and *in vivo* analysis (SA 3 and SA 5)

1. Established the *world's largest Fontan anatomy database* of 230 patients (significantly more than what was estimated in the Grant) with varying anatomies. (Patient number is current as of October 11, 2007).
2. Established *world's largest Fontan flow and physiology database* of 230 patients evaluated from PC MRI for providing realistic boundary conditions for experimental and computational fluid dynamic simulations (not proposed in the original Grant). These patient databases are precious, unique and essential for the proposed high-impact clinical pediatric research in CHD management and surgical treatment.
3. Developed image-processing techniques for performing 3D morphological reconstructions from serial anatomic MRI and 3D flow fields from sparse PC MRI measurements.
4. Developed a method to non-invasively evaluate energy losses from PC MRI using the viscous dissipation formulation. This enables clinical monitoring of power loss over the cardiac cycle as a functional parameter.
5. Developed a method for the non-invasive assessment of ventricular output power using PC MRI of the ascending aorta and catheterization pressures. Studied the power output differences between single left and single right ventricles and correlated the results with ascending aorta flow patterns.
6. Developed a skeletonization method for the quantitative analysis of TCPC geometries (including baffle size, curvature, caval offset, flaring and connection angles).

Experimental and Numerical Modeling of TCPC Hemodynamics (SA 1)

7. Developed a novel method for creating patient-specific transparent flow phantoms for *in vitro* experiments using rapid prototyping on models obtained from the 3D MRI reconstruction of the patient's TCPC. Conducted multimodal *in vitro* experiments including power loss, dye flow visualization, and particle image velocimetry (PIV) on patient-specific models across all TCPC and BCPC templates.
8. Conducted *in vitro* PC MRI experiments for validation against PIV and CFD. Results yielded a good match.
9. Developed new registration techniques for multi-modal validation of PC MRI, PIV, and CFD.
10. Developed an accurate CFD simulation methodology using two commercially available codes (Fluent and Fidap). Using this technology, hemodynamic analyses of a large number of patient-specific cases (about 40) have been completed. CFD validation studies with PIV (2D and 3D) have been completed successfully assuring credible computational hemodynamic analysis.
11. Developed an in-house CFD code capable of running unsteady simulations in complex Fontan pathways.
12. Derived a proper normalization for power losses for removing patient-to-patient variations. This allowed the establishment of definite trends even with relatively small sample sizes.
13. Derived an analytical expression for the theoretical (and non invasive) prediction of power losses based on TCPC vessel dimensions and flow rates.

Modeling Applied to Fontan Patient Studies (SA1 and SA4)

14. Correlated power loss evaluated from CFD at exercise flow conditions with VO_{2max} measured from clinical exercise studies. This unique study is our first effort linking clinical parameters to CFD modeling.
15. First research group that numerically modeled the feasibility of a pediatric venous ventricle assist (pVAD) in the Fontan circulation.
16. Detailed hemodynamic analysis of three fundamental Fontan templates including intra atrial, extra cardiac, and Fontans with bilateral SVCs, using CFD, *in vivo* PC MRI, and *in vitro* experiments.
17. Compared the hemodynamic performance of Hemi-Fontan with Glenn type connections, which has long been questioned by the surgical community.
18. Analyzed the differences in pre and post-Fontan hemodynamics for 5 patients using CFD. Hemodynamic changes were compiled over the surgical timeline.
19. Developed lumped parameter models to model/simulate the effects of respiration and exercise on the single ventricle circulation.
20. Simulated the effects of IVC fenestration. In addition, the effects of LPA stenosis was quantified over the complete physiological operation range through ~200 CFD simulations.
21. Computed the hepatic blood distribution in 15 patient-specific anatomical models using 3D CFD.

Animal studies (SA2)

22. Demonstrated that Fontan circulations can be created in 10-20 Kg lambs via TCP type connections in concert with single ventricle physiology without the use of assist devices.
23. Designed a new TCPY connection for redirecting the SVC and IVC flow in a parallel fashion to the pulmonary circulation that will be optimal in patients with appropriate anatomy.
24. Demonstrated the impact of respiration rate and stroke volume in animal models with a Fontan circulation. Results clearly indicated the high impact of respiration with the energetics varying as much as 100% with small changes in parameters.
25. The animal studies provided boundary conditions and validation data for lumped parameter (LP) modeling. Validated LP models of the entire circulation provided valuable insights into the acute effects of the Fontan operation. Of particular note, changes in resistances orchestrated the inverse relationships in pressure and flow while changes in extra-luminal pressures caused pressures and flows to go up and down in concert. Both are needed to model the timing effects observed in animal studies.
26. Studied the impact of different graft materials on TCPC performance through CFD models.

Surgical Planning (SA4)

27. Proposed a novel TCPC geometry, Optiflo®, resulting in the lowest energy loss to date (42% lower) in a 2 inlets - 2 outlets configuration. This is critical since we showed that a 7% reduction in power loss is equivalent to 10% acute increase in the cardiac output.
28. Demonstrated the surgical planning concept on two patient-specific cases. This novel approach was featured in the cover of JTCVS in April 2006 issue.
29. Performed a preliminary surgical planning study on 10 patients from the anatomical database using surgeon sketches. A special surgical planning assessment questionnaire was prepared and completed by the 5 cardiac surgeons involved to identify the sources of variation in post-surgical anatomies.
30. Developed an anatomy editing tool SURGEM® allowing surgeons to easily modify existing BCPC or TCPC anatomies to perform virtual surgeries on a computer. This was applied to a parametric study of the 2nd stage, comparing Glenn and hemi-Fontan procedures, and to the 3rd stage, where surgeons were asked to design different TCPC configurations for a given pre-surgical anatomy. Studying these options in CFD allowed for performance comparison and identification of the optimal surgical design.
31. Applied the surgical planning framework in clinical setting, to help determine the best surgical option for 7 patients with severe pulmonary arterio-venous malformations[1]

From the above listed accomplishments it can be seen that we made significant progress in SA1 through 4. As the budget was reduced from what was initially requested, limited progress was made in SA5. This decision was made in consultation with Dr. Gail Pearson, technical monitor of the Grant. Significant progress was made in additional directions, such as the establishment of a large Fontan PC MRI flow database, invention of a new optimized Fontan connection, and development of an in-house CFD code for a more accurate simulation of TCPC flow. **29** peer reviewed papers and **3** book chapters have been published, and at least **95** presentations have been made at national and international meetings as a consequence of this BRP. In addition, **1** patent has been applied for, decision for which is pending. In order to accomplish the above SAs and increase our understanding of the anatomy and physiology of the TCPC, significant efforts had to be devoted to tool and model development. The following progress report is organized to reflect these developments in the following order: (1) analysis of the patient MRI and PC MRI scans, (2) experimental and computational models of the TCPC, (3) animal and computational models of the whole univentricular circulation (4) preliminary surgical planning. This section closes with preliminary results needed to lead into the next phase of the Grant.

1.1. *In vivo* MRI and PC MRI Analysis

1.1.1. Anatomic Reconstruction Methodology (Published in IEEE TBME[2], JCMR[3] and IEEE TMI[4])

The first step towards the establishment of our anatomical database was to reconstruct 3D patient-specific anatomies based on stacks of sparsely sampled (due to imaging time constraints) cardiac magnetic resonance (CMR) images (Figure 1-1). Our approach may be split into 3 major steps: a.) Interpolation, b.) Segmentation, and c.) 3D Reconstruction. *Interpolation:* A novel interpolation method known as adaptive control grid interpolation (ACGI) was developed in our lab to achieve an isotropic 3D dataset from non-isotropic serial CMR data[2]. This facilitated a smoother TCPC segmentation and 3D reconstruction. *Segmentation:* After interpolation, the vessels of interest are segmented out of the enhanced MRI dataset, isolating the TCPC structure from the rest of the thorax. In our segmentation approach, the MR image is considered as a 3D map, where the slope is dictated by the intensity gradients of the MRI. Brutal changes in intensity (when going from a vessel lumen to the surrounding tissues for example) appear as steep slopes, whereas regions of uniform intensities appear as valleys. A segmentation element (or ball) is released in the lumen of the vessel of interest and bounces against the steep slopes (corresponding to the vessel walls) until the whole vessel lumen is segmented. A larger ball segments the vessel faster and ensures that the segmentation does not leak into nearby vessels, while a smaller ball could segment much smaller vessels, but has the risk of capturing surrounding regions. In practice, a spherical shape element with a radius of 2.5 pixels was preferentially used, as it was the smallest element that described a spherical profile reasonably well. When this element size proved too small and the ball got out of the vessel of interest, the element size was incremented and segmentation was repeated locally, around the problematic regions. Results demonstrated that using a shape element instead of a single pixel did not sacrifice segmentation accuracy at the hands of feasibility given that our datasets were of sufficient resolution[3]. *3D Reconstruction:* All the segmented slices are imported into Mimics (Materialize, Inc.), which creates a smooth 3D representation of the TCPC. An in-house code was written to automatically transform the given TCPC geometry to the MRI co-ordinate system, such that the PC MRI flow planes are automatically registered onto the anatomy, thus allowing for accurate prescription of CFD boundary conditions. **This anatomic reconstruction approach was successfully applied to 170 TCPC and 60 BCPC anatomies**, as well as to patients' aortas when available. These reconstructed anatomies were classified under the five TCPC templates proposed in the original Grant (Figure 1-3) and two BCPC options (Hemi-Fontan and Glenn).

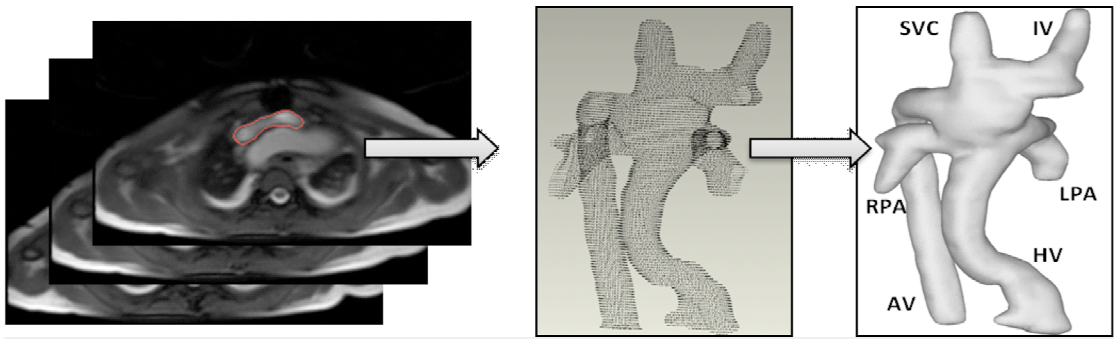

Figure 1-1: Steps for the anatomic reconstruction of the TCPC from the stack of axial MRI. a) The TCPC is first segmented in each slice; b) The segmented contours are then imported into Geomagic Studio 9.0 (Geomagic Inc., NC, USA); c) A smooth surface is fitted to the points to obtain a 3D anatomic reconstruction of the TCPC.

1.1.2. Velocity Segmentation and Reconstruction Methodology (published in JBME[5], 2 submitted to JMRI[6] and to Experiments and Fluids[2], 2 articles in preparation)

As part of the MRI protocol, the three centers involved in the study (i.e. CHOP, CHOA, and UNC) acquired CINE PC MRI in addition to the anatomic MRI stacks. Particular emphasis was placed on imaging the IVC, SVC, LPA and RPA as well as the ascending aorta. One slice per vessel was acquired orthogonal to the primary direction of flow to maximize the signal to noise ratio. Due to the limited scan time that was available, a single velocity component (through-plane) was obtained in most of the patients. In situations where there was

more time available, in-plane components were acquired as well. Finally, in a few patients (~30) coronal PC MRI planes were acquired across the IVC baffle to assess the 3D *in vivo* flow fields.

Velocity segmentation[2, 6]*:* The methodology developed for velocity segmentation employs parametric active contours[7] (or snakes), where the user specifies an initial contour that evolves under the influence of internal and external energy fields to precisely sit on the vessel border. The algorithm was modified to use Gradient Vector Flow, which is an improved method for evaluating energy fields[8]. Flow artifacts, introduced by air in the lungs, are eliminated with an adaptive median filtering approach, where spurious noise vectors are automatically removed close to the vessel border. The technique was validated against manual segmentation for 15 patients randomly selected from our database (Table 1-1), showing an excellent agreement between the two methods. **230 patient PC MRI flow data were segmented,** providing velocity cross-sections that can then be used as input boundary conditions for computational and experimental analysis.

Vessel	AS Flow (L/Min)	MS Flow (L/Min)	% Diff	AS Area (cm^2)	MS Area (cm^2)	% Diff
Aorta	3.20 ± 1.54	3.21 ± 1.49	-0.32	7.26 ± 3.58	7.12 ± 3.51	1.99
IVC	1.88 ± 0.99	1.89 ± 1.00	-0.93	4.19 ± 2.90	4.36 ± 3.26	-3.82
SVC	0.92 ± 0.32	0.92 ± 0.24	-0.24	1.88 ± 1.24	1.84 ± 1.15	1.87
LPA	1.22 ± 0.81	1.22 ± 0.78	0.63	1.76 ± 1.09	1.62 ± 0.95	8.27
RPA	2.08 ± 0.76	2.12 ± 0.79	-1.92	3.51 ± 1.46	3.54 ± 1.62	-0.69

Table 1-1: Validation of the automated segmentation (AS) against manual segmentation (MS) results.

Volumetric Flow Field Reconstruction: The ability to visualize the 3D *in vivo* blood flow structures throughout the cardiac cycle would provide a strong diagnostic tool for the assessment of pathology. In particular, for patients born with single ventricle defects, this would allow clinicians to assess how well the TCPC is performing. Towards this end, a new method was developed that utilizes blood flow incompressibility to reconstruct the continuous 3D velocity fields of the TCPC from sparse coronal PC MRI measurements. In order to accomplish this, the following are required:

a.) 3D representation of the vessel anatomy
b.) Measurements of all 3 components of velocities inside the vessel over one cardiac cycle
c.) A model for zero divergence interpolation of the measured 3D velocities onto the 3D anatomy

For a), the anatomy is reconstructed using the anatomic reconstruction methodology described in Section 1.1.1. For b), a stack of 3D retrospectively triggered PC MRI slices is acquired in the coronal direction with a matrix size of 320 x 230 pixels, a resolution of 1.25 m^2, a slice thickness of 6 mm, and 20 cardiac phases. Using the segmentation from a) the velocity measurements inside the vessel of interest are retained, and the rest are discarded. For c) a divergence free interpolant is initialized as depicted in Equation 1-1 to Equation 1-3, where V(x) is the velocity field expressed as a function of the location inside the flow domain. Φ (x) is a matrix valued radial basis function that can be used for a continuous flow field representation in the TCPC, c_j are the vector-valued interpolating coefficients that can be estimated based on the least-squares approach, and α is a scaling parameter that is dependent upon the control point spacing.

Equation 1-1

$$V(\vec{x}) = \sum_{j=1}^{p} \Phi\left(\left|\vec{x} - \vec{x}_j\right|\right)\vec{c}_j$$

Equation 1-2

$$\Phi_\alpha(x) = \left\{-\Delta I + \nabla\nabla^T\right\}\varphi_\alpha(x)$$

Equation 1-3

$$\varphi_\alpha(x) = e^{-\alpha\|x\|^2}$$

To enforce the no-slip condition, the velocity along the vessel boundary is assigned to be 0. It can be seen that mathematically the divergence of the radial basis function is equal to 0. Once all c_j are estimated, they can be used to evaluate the velocity field anywhere in the TCPC geometry. Figure 1-2 provides a reconstruction example, with 7 original PC MRI slices registered onto the corresponding anatomy, and the resulting reconstructed 3D velocity field (shown as stream-traces in the figure). Notice the intense recirculation region in the center where the IVC connects to the BCPC.

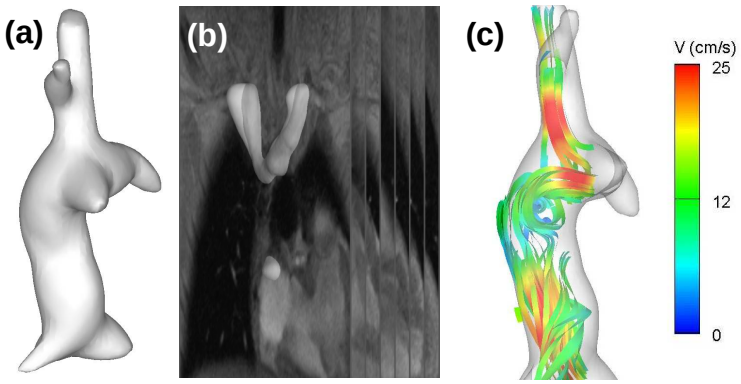

Figure 1-2: Various steps involved in the 3D velocity field reconstruction. a) TCPC geometry reconstructed from MRI, b) PC MRI planes registered onto the TCPC, c) Coronal view of the 3D stream lines reconstructed using divergence-free interpolation.

1.1.3. Anatomic & Velocity Database

One of the major accomplishments of this BRP Grant was the establishment of the largest anatomic and flow database of Fontan patients (to our knowledge). As of now, this database contains a total of 230 anatomic reconstructions comprising 170 completed Fontan (see Figure 1-3 for configurations and patient numbers of the 5 TCPC templates proposed in the original Grant proposal), and 60 BCPC anatomies comprised of 49 bidirectional Glenn and 11 hemi-Fontan templates. Please note that there were 31 TCPCs whose clinical data was unavailable for accurate classification into one of the 5 templates. In addition the ascending aorta of 12 patients was reconstructed to study the impact of ascending aorta geometry on single ventricle hemodynamics. This database has largely exceeded our original expectation of 120 patients for 5 years. The reconstructed flows and anatomies of most of these anatomies are available to all the collaborators of the Grant and can be readily accessed via a secure website (http://fontan.bme.gatech.edu) with a username and password provided by the system administrator. For the first time, surgeons can easily access and visualize a large database of anatomies, pinpointing recurrent features and seeing other surgical alternatives. Preliminary statistical analyses were conducted to compare the dominant geometric characteristics of intra-atrials and extra-cardiacs, or the relative contribution of different vessels to the total flow for different TCPC templates. Finally, such anatomical and flow information will be key factors in the proposed renewal to develop our surgical planning tools and model the required post-operative hemodynamic parameters.

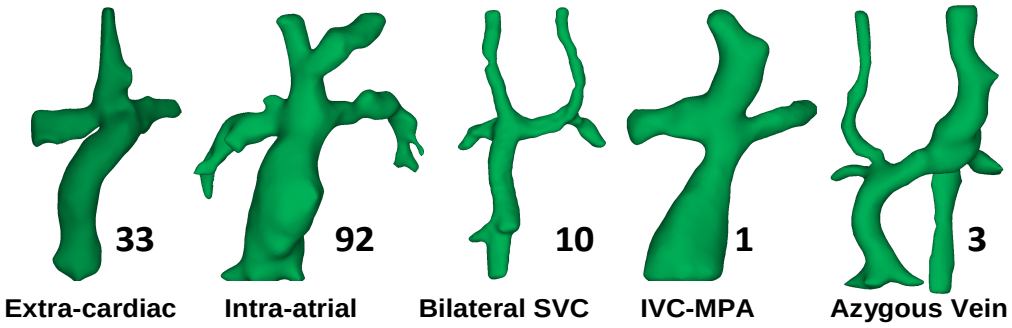

Figure 1-3: TCPC templates representative of the current anatomical database, with numbers of available reconstructions indicated on the side. In addition to these 5 TCPC templates, our database also includes 49 Glenn and 11 Hemi-Fontan reconstructions.

1.1.4. Fontan Website

In order to provide widespread access to the collected data, significant work has been done towards the establishment of a database, storing anatomical as well as all subsequent experimental and numerical data obtained for each patient. The thus-established database is accessible via a secured website, whose usernames and passwords can only be delivered by Dr Yoganathan's laboratory. All data are anonimized, and patients appear under codename CHOP XXX or CHOA XXX depending on the origin of the MRI data. The URL is: http://fontan.bme.gatech.edu. Some of the features that were implemented are listed below:

a.) Security of the data
b.) Easy navigation through different projects
c.) Improved visibility of the velocity and flow data
d.) Search capabilities
e.) Provision for storing CFD and experimental data
f.) Improved GUI
g.) Capability to store large sized images and videos

The project listing and search bar enables quick access to the specific clinical cases the user is looking for. When the user clicks on the 'View' tab, it takes him to the page displaying the details of the project. Instead of all the information being displayed in the same page, the display has been segregated into various tabs. The user can easily navigate through the entire project by just using these tabs. Another new addition is the provision to store CFD and experimental results. Once the entire website has been updated and respectively populated with the necessary information, the user will be able to view the complete results of the specific patient case study.

1.1.5. In vivo Analysis

1.1.5.1. Analysis of Geometric Characteristics (2 articles submitted to ATS[9, 10])

To characterize the complex 3D geometries of the TCPC, a skeletonization approach [11-17] was employed to extract the skeleton of the TCPC, which in turn allowed for the quantification of geometric characteristics such as cross-sectional area variation, curvature, and vessel offsets. This methodology was first applied to 26 patients from our database (13 extra-cardiac and 13 intra-atrial TCPCs). This demonstrated that: a) intra-atrials had significantly higher area variations than extra-cardiacs, due to the more irregular geometry of intra-atrial baffles when compared to the smooth extra-cardiac grafts, and b) patients with hypoplastic left heart syndrome (HLHS) were at higher risk of LPA narrowing than those without due to the aortic reconstruction done in the 1st stage. This study was the first to benchmark the anatomic variability of patient specific TCPCs. In addition, such geometric characterization is critical to correlate hemodynamic performances with geometric features.

1.1.5.2. In vivo TCPC Flow Analysis (Submitted to JTCVS[18])

No large series exists that establishes the flow distributions in Fontan patients, which would be an important resource for everyday clinical use and may impact future surgical procedures. A preliminary study was

conducted on 105 randomly selected patients from the current database. Table 1-2 summarizes the results of the Fontan flow analysis. Throughout all templates, the IVC contributed significantly more (59±15%) to the systemic venous return than the single or dual SVC flows combined. Looking at pulmonary flow splits, there was no statistical difference between the right and left pulmonary flows irrespective of the template. In patients with bilateral SVCs, the right SVC had significantly more flow than the left, with a Q_{RSVC} / (Q_{RSVC}+ Q_{LSVC}) ratio of 55±8.9%, but this did not translate in significant difference in blood flow to each lung. There was no significant effect of SVC anastomosis type on pulmonary blood flow in this study, though there was a trend toward TCPCs with hemi-Fontan having slightly higher blood flow to the RPA than those with bidirectional Glenn (56% vs. 51%). BSA in bidirectional Glenns was significantly lower than the hemi-Fontans, which reflects recent surgical trends observed in the timing of these surgeries. The IVC fraction positively correlated with age and BSA (r=0.60 and 0.74, respectively, p<0.05) similar to normal children. Conversely, there was no correlation between RPA fraction of pulmonary blood flow and BSA. Total pulmonary flow was measured at 2.4±0.7 l/min/m^2, compared to 2.8 L/min/m^2 for the measured total caval flow. The mean difference of 0.4 L/min/m^2 (14%) is statistically significant, with a p-value of less than 0.001. Furthermore, pulmonary blood flow was significantly less in intra-atrials compared to extra-cardiacs. A potential explanation for this difference would be the presence of significant aortopulmonary collaterals. More investigation is required to determine the source of differences between aortic flow and systemic blood flow. This data provides a reference for baseline conditions for computational studies. Future studies will focus on the effects of respiration and the effects of exercise on caval and pulmonary blood flow. This information is important when simulating exercise conditions, since accurate flow splits may affect the validity of our simulations.

Flows in l/min/m^2	No LSVC	With LSVC	LSVC vs. No LSVC	Intra-atrial (IA) Fontan	Extra-Cardiac (EC) Fontan	IA vs. EC
n	90	15		69	28	
	Mean±S.D	Mean±S.D	P-value	Mean±S.D	Mean±S.D	P-value
Age	11.0±5.8	14.8±6.9	0.03	11.9±5.5	8.5±4.9	0.005
BSA	1.13±0.44	1.41±0.55	0.03	1.2±0.5	0.9±0.3	0.003
(IVC+SVC)/BSA	2.9±1.0	2.7±0.8	0.61	2.8±1.0	3.0±1.0	0.43
(RPA+LPA)/BSA	2.5±0.8	2.2±0.6	0.17	2.3±0.8	2.7±0.8	0.03
IVC/(IVC+SVC)	0.59±0.15	0.61±0.11	0.59	0.60±0.15	0.55±0.11	0.17
RPA/(RPA+LPA)	0.55±0.13	0.50±0.16	0.22	0.55±0.13	0.51±0.13	0.14
(RPA+LPA)/ (SVC+IVC	0.92±0.2	1.1±1.7	0.38	0.88±0.3	1.26±1.9	0.1

Table 1-2: Flow comparisons between intra-atrial and extra-cardiac Fontan connections.

1.1.5.3. Differences in flow dynamics between different single ventricle morphologies (published in ATS[19])

Many of the studies conducted in our lab have looked at evaluating the power loss of the TCPC. However, a power loss value does not have much significance if the input power supplied by the single ventricle is unknown. Towards this end, we have developed a simple method for evaluating single ventricle output power from PC MRI acquired in the ascending aorta using the modified Bernoulli's equation[19, 20]. The exact formulation is provided in Equation 1-4, where ρ is the blood density (1060 kg/m3), v the mean systolic velocity, P_{mean} the mean static pressure, and $Q_{mean(systole)}$ the mean systolic flow rate evaluated from PC MRI. In order to evaluate this equation, the mean arterial pressure (MAP), which is clinically defined as a weighted average of the cuff pressure, was used as the static pressure. Evaluating the power output of the ventricle allows for comparison of power capacities of different single ventricle patients and can be used in the context of TCPC energy dissipation to put the energy loss in perspective of the single ventricle.

Equation 1-4

$$\dot{E} = \left(\frac{1}{2} \rho \cdot v_{systole}^2 + P_{mean} \right) * Q_{mean(systole)}$$

This approach was applied to a subset of 36 patients from our current database for whom. cuff blood pressure had been recorded either just before or just after the imaging was done. These patients were further subdivided into two groups: the HLHS group consisted of 18 patients diagnosed with HLHS while the non-HLHS group consisted of the other variants of single ventricle patients. Of the 18 with HLHS, 15 had undergone a Fontan operation, 2 a bidirectional Glenn procedure and 1 hemi-Fontan. The non-HLHS group consisted of 14 patients who had undergone the Fontan operation, and 4 who had a bidirectional Glenn procedure. 28/36 patients were from CHOP and the rest from CHOA. PC MRI was performed on all of these patients approximately 2-4 mm above the aortic valve. The computed power was indexed using BSA for ease of comparison across all patient sizes. Results are shown as part of Figure 1-4. HLHS patients had significantly lower output power and cardiac index than non-HLHS patients. When correlated with the flow profile seen in the AAo, output power correlated negatively with non-uniform flow profiles (p-value<0.05). Most HLHS patients undergo an aortic arch reconstruction, which was observed to yield non-uniform flow directly above the aortic valve. **This suggested that children with aortic arch reconstruction had lower ventricular power output than those without**.

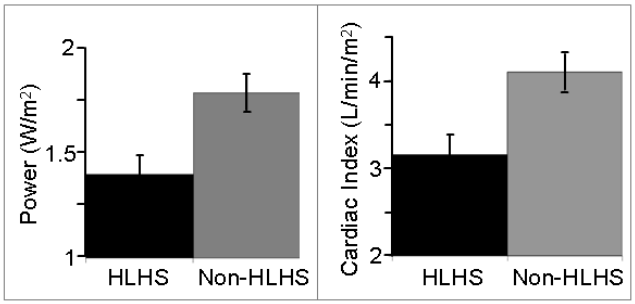

Figure 1-4: Comparison of output power and cardiac index for HLHS and non-HLHS patients

1.2. Models of the TCPC Hemodynamics

Major methodology development milestones were accomplished during this BRP enabling patient-specific studies, in order to: (a) better understand TCPC flow dynamics and; (b) optimize surgical design for each individual patient. Four main hemodynamic parameters have been retained to assess the efficiency of alternate TCPC procedures, namely power loss across the connection as a global measure for efficiency, pulmonary flow split for lung perfusion, hepatic flow distribution for lung development, and finally detailed flow structure analysis to identify the sources of energy dissipation. A multi-modality protocol was established to assess each of these aspects (Figure 1-5). 3D anatomy and flow reconstructions were obtained from patients' MRI and PC MRI (Section 1.1) and utilized for both numerical and experimental studies. The methodologies adopted for performing each of these studies and the corresponding results are detailed in the following sections.

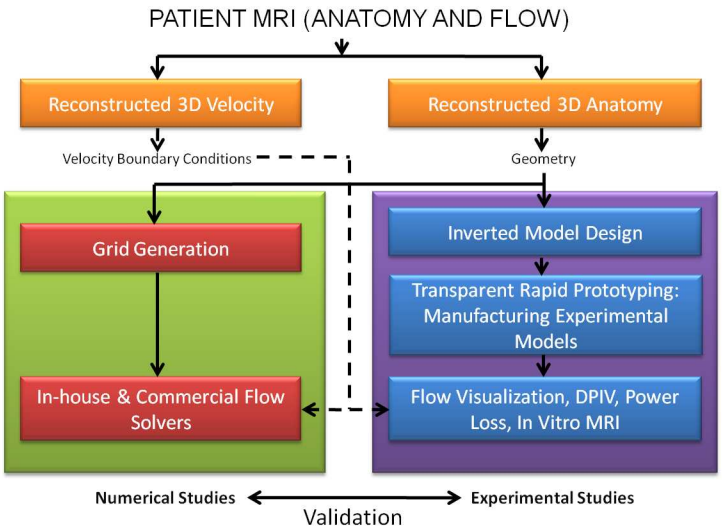

Figure 1-5: Overview of the experimental and numerical methodology.

1.2.1. ***Experimental In Vitro Modeling (Published in JBME[21], ATS[22] and JTCVS[23], 1 in preparation)***

In vitro experiments were conducted to: (1) validate numerical simulations, (2) validate PC MRI measurements, and (3) provide insights into the TCPC hemodynamics. Special attention was thus paid to manufacturing models with a thorough geometric control, developing a multimodal experimental approach to acquire all data necessary for validation, and carefully choosing the TCPC templates under investigation.

In vitro Model Manufacturing[21]*:* The first step was to succeed in manufacturing anatomically accurate transparent replicas of the TCPC. Traditionally this was achieved by reverse engineering the morphology of interest through tedious casting/curing operations, ultimately producing a transparent Slygard enclosure of the TCPC lumen. For the small, complex pediatric anatomies and the large number of,experiments needed, this process was found to be expensive and difficult to apply. To circumvent these issues, another path was adopted, where the TCPC model was inverted using computer aided design (CAD) and the physical model was built directly via rapid prototyping using transparent stereolithographic resins. This approach presented the following advantages: (i) it is very accurate allowing the creation of identical experimental and CFD models that are crucial for CFD validation; (ii) it is cheaper than the original proposed method; (iii) it is time-effective with the entire design and manufacturing process taking no more than 1 or 2 days for up-to 6 models manufactured in one batch. Figure 1-6 summarizes our manufacturing protocol applied to a patient-specific TCPC.

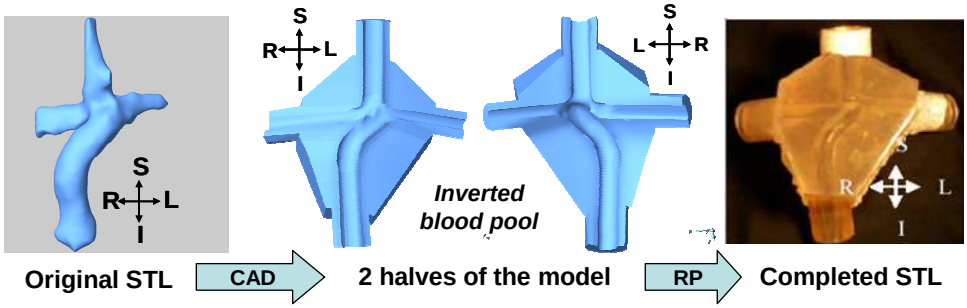

Figure 1-6: In vitro TCPC model generation for an extra-cardiac connection from CAD to phantom model.

Experimental Protocol: All experiments were conducted in a steady flow rig at GT (Figure 1-7)[24, 25]. To fully characterize the different operating conditions of the TCPC, detailed experiments were conducted with flow rates ranging from baseline resting condition (taken as the PC MRI flow rates) to exercise condition (taken as 2 to 3 times the PC MRI flow rates). The caval flow splits were set according to the *in vivo* flow split, while the pulmonary flow splits were varied over the entire physiologic range: from 30/70 to 70/30 LPA/RPA. The experimental protocol included the systematic acquisition of pressure and flow rate at each inlet and outlet for the subsequent power loss computations, high-speed flow visualization (Figure 1-7), and particle image velocimetry (PIV). Selected models were also explored by laser-Doppler velocimetry for its high temporal resolution (2 models) and by PC MRI to assess the accuracy of PC MRI measurements in TCPC geometries (6 models). These methods were complementary and used in combination for a multi-modal validation campaign.

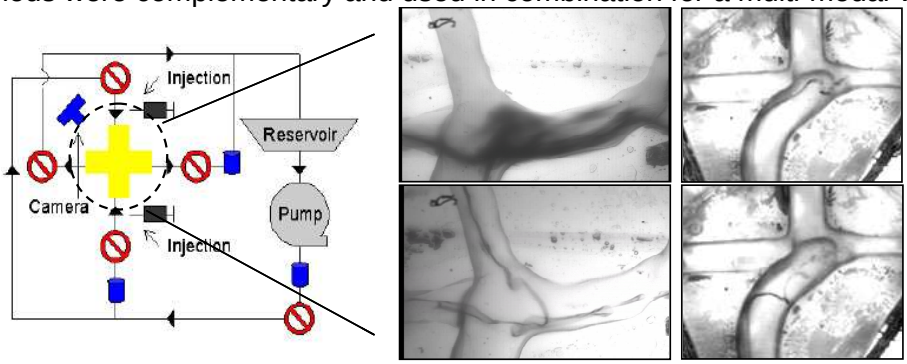

Figure 1-7: Flow loop setup and flow visualization videos of extra-cardiac connections with single (Right) and dual (Middle) SVCs

Summary of experimental effort (2 publications [22, 23], 1 in preparation)*:* Patient-specific *in vitro* studies have been carried out on 6 BCPC (3 Glenn and 3 Hemi-Fontan) and 9 TCPC anatomies, spanning four TCPC templates: extra-cardiac (4, among which 1 with bilateral SVCs), intra-atrial (4), and IVC-to-MPA (1). Cases with interrupted-IVC and azygous continuation have not been modeled experimentally due to the complexity of model generation and experimental setup. Special attention was paid to comparing intra-atrial with extra-cardiac TCPCs (n=8) and Hemi-Fontan with Glenn BCPCs (n=6). These comparative *in vitro* studies were required to determine the hydrodynamic advantage of one basic template relative to the other. Initially, the small sample sizes were not sufficient to draw statistically significant conclusions, but did demonstrate some trends that have later been confirmed through systematic CFD simulations. We have shown that, under steady flow conditions, extra-cardiac TCPC and bidirectional Glenn yielded lower power losses than intra-atrial TCPC[26], and hemi-Fontans of equivalent vessel dimensions due to the smoother flow fields observed in the former templates. However, parametric *in vitro* experiments on idealized glass models (9 models total) have confirmed that the major factors influencing power loss are vessel dimensions and the presence of large mismatches in diameters, such as those observed when small PA's connect to large intra-atrial pouches. Overall, a significant insight into TCPC flow dynamics was attained via *in vitro* experiments that resulted in 3 publications in leading clinical journals (ATS, JBME, JTCVS).

1.2.2. 3D Computational Fluid Dynamics (CFD) Modeling

The CFD effort may be separated into two major branches: (1) developing and validating our simulation methodology; (2) conducting parametric and patient-specific simulations. CFD studies were performed on a large number of TCPC anatomies (~40 models), idealized parametric models (~75 models) as well as 2nd stage BCPC anatomies (7 models).

1.2.2.1. CFD Validation

CFD simulations provide a full, 3-D description of the flow and pressure field, enabling a fundamental understanding of the complex TCPC hemodynamics. However, prior to drawing any conclusion and any surgical implication from the numerical studies, a prerequisite is to ensure their reliability. Validation of the CFD simulations against their experimental counterparts is integral to our methodology and has been completed for the 3 major TCPC templates, and for all of the idealized geometries.

Steady state Studies and Time-Averaged parameters – published in ABME[27] and JBME[28]: In the original Grant proposal, all CFD studies were to be conducted using the commercial code FIDAP (ANSYS Inc.), which is of sufficient accuracy to model blood flows with low Reynold's numbers in smooth cardio-vascular geometries. However, despite steady and laminar inflows, the first *in vitro* experiment in a patient specific model (Figure 1-8 A-C) revealed unexpectedly complex flow features involving flow instabilities and transitions from laminar to turbulent regimes[22, 24], which FIDAP failed to capture with a practical time-step and mesh resolution (Pekkan et al.[27]). This observation lead to the development of advanced CFD tools taking flow unsteadiness into consideration.

Transient Studies on Unsteady TCPC Flows - ABME[29]: To account for the observed flow unsteadiness, the CFD package FLUENT (ANSYS Inc., NH) was used as it possesses a second order upwind scheme option. A collaboration was also established with the ANSYS/Fluent development team in order to enhance the accuracy of the flow solver by applying the latest Tet/Hybrid Hex-core meshing scheme. Two anatomical models were studied and an excellent agreement was established between unsteady PIV, LDV, and CFD (Figure 1-8 D).

Development of an In-House High-Order Transient Flow Solver – (Published in Computers and Fluids [30]): Our experience with commercial CFD packages underscored the need for pursuing the development of an in-house high-resolution CFD code in tandem with commercial code studies. The advantage of an in-house code is that it can be optimized for TCPC flows, for a more accurate and efficient simulation. Moreover, it permits access to the source code, thereby facilitating the surgical planning and optimization of the TCPC. In structured immersed boundary (IB) methods, the complex boundary is immersed in a Cartesian background mesh. The Navier-Stokes equations are solved only on the grid nodes falling within the flow domain, while those falling outside are disregarded from the computations. For the fluid nodes in the immediate vicinity of the vessel wall, the solution is reconstructed via interpolation. However, for our purposes the complexity of the *in vivo* cardiovascular geometries results in a large number of "unused" nodes residing outside of the fluid domain. This imposes a large memory and computational overhead, thus limiting the applicability of structured IB approaches to clinical studies. An unstructured IB method was thus developed that solely retained the Cartesian grid nodes that fall within the flow domain. The code was validated against experimental data for

cases of increasing complexity, going from a 90 degree curved pipe to idealized and patient-specific TCPC, Figure 1-8. In all cases, time-averaged velocity fields and profiles were in good agreement with the experimental data. Coupled with the flow solver developed by Dr Sotiropoulos at the University of Minnesota for pulsatile simulations in aortic heart valves, this approach will provide a robust technique to handle phasic TCPC flow simulations proposed for the renewal.

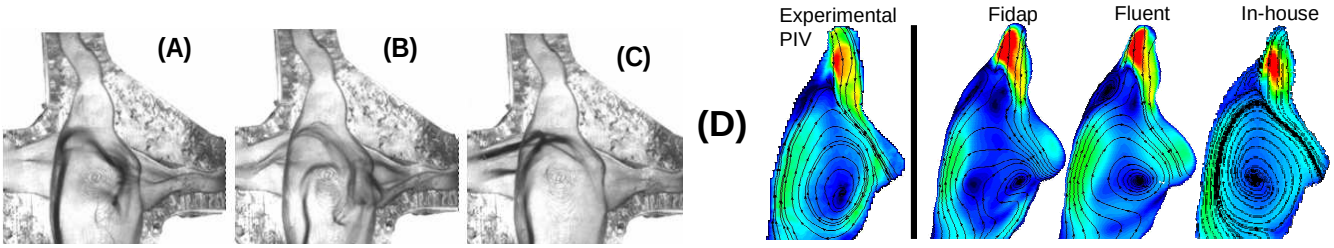

Figure 1-8: (A-C): Flow visualization, highlighting the flow instabilities within the baffle. The dye was injected at the exact same location for all 3 snapshots. (D): Comparison of time-averaged in-plane velocity magnitudes: PIV vs. CFD (1st order Fidap, 2nd order Fluent and in-house

1.2.3. Example of Hemodynamic Analyses & Their Clinical Relevance (Combined Experimental and CFD Results)

The focus of the past years was mainly technology development oriented. As such, experimental and numerical investigations have been limited to a subset of the constituted patient database. Special emphasis was set on the type of analysis that could be performed and potential clinical benefits. The subsequent section reports our preliminary efforts in that direction. Patient-specific *in vitro* studies have been carried out on 9 TCPC anatomies, spanning four TCPC templates: extra-cardiac (4, among which 1 with bilateral SVCs), intra-atrial (4), and IVC-to-MPA (1). Cases with interrupted-IVC and azygous continuation have not been modeled experimentally due to the complexity of model generation and experimental setup. CFD studies were performed on a large number of idealized parametric models (~75 models) and patient-specific TCPC anatomies (~40 models). Results from all approaches are listed below, grouped by the specific geometric parameter.

1.2.3.1. 2nd stage BCPC: Glenn vs. Hemi-Fontan (published in ABME[31])

A major area of surgical interest is to understand the hemodynamic differences between different surgical options at the second and third stage of the Fontan operation. For each one of them, at least two different options are routinely used, mainly dictated by surgeons' preference, but the hemodynamic advantage of one surgical design over another has not yet been determined or published. Focusing on the BCPC, a comparative study of bidirectional Glenn and hemi-Fontan was conducted using both patient-specific and idealized geometries. 3 Glenn and 3 hemi-Fontan anatomies were compared using experimental and CFD simulations. **Error! Reference source not found.** shows the results of a sample Glenn and hemi-Fontan geometry. To draw more general conclusions, a parametric study was then conducted in CFD using both idealized and anatomical geometries. For the anatomic parametric study, two anatomies of similar vessel dimensions were selected and modified using our newly developed surgical planning tool, Figure 1-17. In summary, presence of stenosis at the SVC anastomosis or along the vessels was found to be the most critical parameter in increasing power loss, while pouch size and flare shape were insignificant. However, for identical vessel dimensions, the power losses associated with idealized and patient-specific Glenns were 83% (p=0.08) and 62% lower than those measured in hemi-Fontan, respectively. This was attributed to the anterior-posterior caval offset present in hemi-Fontan connections which results in a bulgy area with flow recirculation and, in turn, increased energy dissipation.

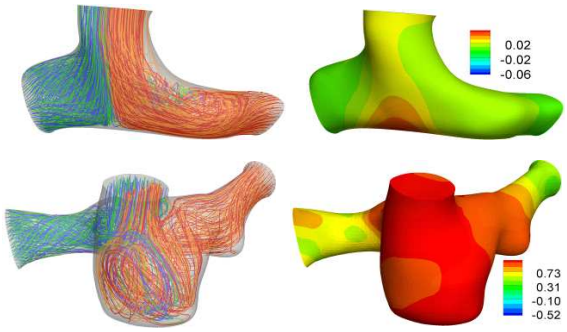

Figure 1-9: Comparison of hemodynamics between bidirectional Glenn (Top Row) and hemi-Fontan geometries (Bottom Row). On the left are the trreamtraces color coded by those going to the LPA (red) and RPA (blue). On the right are the pressure contour maps

1.2.3.2. 3rd stage TCPC: Intra-Atrial vs. Extra-Cardiac

For the 3rd stage, the two most commonly used options are intra-atrial and extra-cardiac connections. In an effort to better characterize the characteristics and resulting hemodynamics of the two alternatives, a multi-modality approach was under-taken combining *in vitro* experiments and 3D CFD simulations. Results from all approaches are listed below, grouped by the specific geometric parameter.

PA stenosis as the driving factor for high power losses (Circulation[32], JBiomech [33], JTCVS[34]): A retrospective study was conducted on 22 patients (11 extra-cardiacs and 11 intra-atrials). Power losses across the TCPC were available from *in vitro* experiments and CFD simulations for 5 and 9 of the 22 patients, respectively. To remove patient-to-patient variability, power losses were normalized by $\rho CO^3/BSA^2$, where CO is the cardiac output and BSA the body surface area. Cardiac index (CI) data was available for all patients and geometric parameters were extracted using a skeletonization approach. The analysis revealed that the predominant factor for TCPC dissipation was the minimum PA cross-sectional area (R^2-value of 0.898 and P<0.0002, as shown in Figure 1-10(A)), while all other geometric features, including connection type, had lesser influence. In addition, as shown in Figure 1-10(B), CI is strongly dependent on the minimum PA area (P=0.006) suggesting that TCPC energy loss has a significant impact on cardiac output. This correlated well with earlier clinical findings showing that PA stenosis decreased flow efficiency and increased the risk factor for Fontan failure[35].

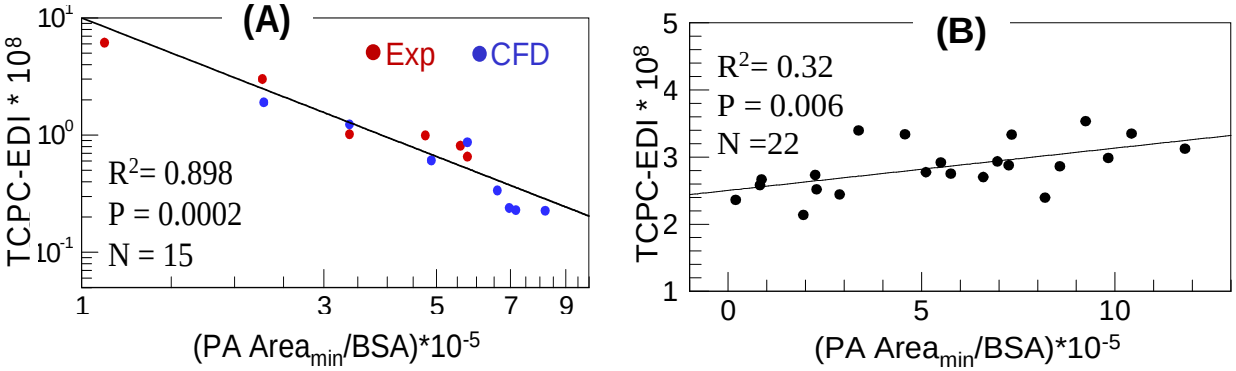

Figure 1-10: (A) Normalized Power loss vs. normalized minimum PA area and (B) Cardiac Index vs. normalized minimum PA area.

Investigating further, parametric CFD studies conducted on idealized geometries have demonstrated that diffuse stenosis was less severe than discrete stenosis. A diffuse stenosis, obstructing less than 60% of the vessel lumen, resulted in less than 12% decrease in left lung perfusion, while a discrete stenosis that did not obstruct more than 40% of the vessel lumen was within the same clinically tolerable levels of lung performance.

Formal relationship between TCPC geometry and associated power losses (J Biomech[33]): A number of experimental and numerical studies have investigated the impact of individual parameters on TCPC efficiency. However, due to the wide variety of anatomy and flow conditions tested, the relative impact of each of these parameters is difficult to assess. The above systematic analysis of PA stenosis opened the avenue for a more formal formulation that would link parameters together in a mathematical formulation. We thus developed a simplistic and clinically useful mathematical model of the dependence of energy dissipation on the governing flow variables; namely, cardiac output, flow split, body surface area, Reynolds number, and certain geometric characteristics. *In vitro* energy loss data corresponding to six patients' anatomies validated the predicted dependency of each variable and were used to develop a predictive, semi-empirical energy dissipation model of the TCPC. It was shown that the resistance of the connection depended on Reynolds number and geometrical factors alone. Energy dissipation was established to be a cubic function of pulmonary flow split in the physiological range, and to strongly correlate with minimum PA area as a power law decay with an exponent of -5/4 (R^2>0.88) under exercise conditions. Further studies with larger sample sizes are necessary for incorporating finer geometrical parameters such as vessel curvatures and offsets.

Quantification of Hepatic Flow Distribution (Submitted to JTCVS): *In vivo* PC MRI data show that flow rates to the LPA and RPA are not statistically different irrespective of the TCPC template under consideration. However, a balanced LPA/RPA flow split per se is not sufficient for proper lung development, and development of unilateral PAVMs after completion of the Fontan circulation has been widely reported[36-40]. These malformations are intrapulmonary arterial-to-venous shunts, which bypass the gas exchange units, resulting in decreased oxygen saturation and increasing cyanosis. Although the underlying mechanism leading to PAVMs is unknown, studies have shown that liver-derived hepatic factors prevent the formation of PAVMs[37, 39-41]. A Lagrangian particle tracking method was thus implemented and applied to CFD results to quantify the portion of the IVC flow directed to the right and left lung. A cross-section of the IVC was uniformly seeded with mass-less particles that were carried by the flow stream. IVC flow distribution was quantified as the ratio of particles exiting through the RPA and LPA. This approach was applied to 12 patient-specific anatomies (8 intra-atrials and 4 extra-cardiacs), demonstrating a more even hepatic flow distribution in intra-atrials than extra-cardiacs ($p<0.05$) due to the flow recirculation and mixing commonly observed in intra-atrials. In addition, hepatic flow distribution did not change markedly between rest and exercise conditions, but this might be due to the fact that pulmonary flow splits were maintained constant between rest and exercise.

Impact of IVC geometry on hepatic flow distribution and pulmonary arteriovenous malformation (published in JACC[1]): One single ventricle subgroup that is especially at risk for PAVMs is children having an interrupted IVC with an azygous vein continuation (Kawashima Procedure)[42]. Their palliation results in a configuration that is much more complex than a typical TCPC geometry. This complexity further confounds the inherent challenges associated with visualizing hepatic flow splits pre-operatively based on geometry alone, which make it difficult to identify the surgical option that will distribute the hepatic flow "equally" to both the lungs. Preliminary studies were thus conducted, using an interactive surgical planning interface coupled with our fully validated CFD framework to determine which TCPC geometry would achieve equal hepatic flow distribution (HFD). A 4 year old patient with severe PAVMs presented to CHOP having oxygen saturations in the low 70's. The patient previously had a Kawashima procedure, with an extra-cardiac Fontan connection. HFD to the right lung significantly correlated with PAVMs observed in the contra-lateral lung (Figs. 4.07 and 4.08). The patient underwent cardiac magnetic resonance imaging (CMR) for 3D anatomy and flow reconstruction. Of the multiple options that were investigated, an IVC to azygous vein conduit best improved the hepatic flow split (Fig 4.08). The surgery was performed using this approach, and five months after surgery, oxygen saturations were up from 68% to 90% demonstrating the closure of PAVMs. This study underscores the need for a proper understanding of the hemodynamic parameters at stake, which will then allow for proper planning and design of the TCPC. It also demonstrates the potential of a properly tuned numerical model for the investigation of different treatment options. The current proposal will establish the fundamental, but missing, link between TCPC hemodynamics, ventricular function and patient well-being, enabling sophisticated surgical and clinical planning further down the road.

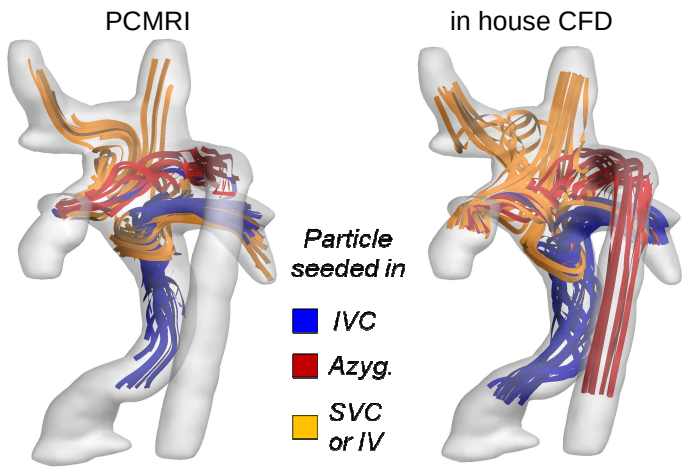

Figure 1-11: Comparison of the in vivo (PCMRI) and simulated (CFD) flow fields in the original failing TCPC

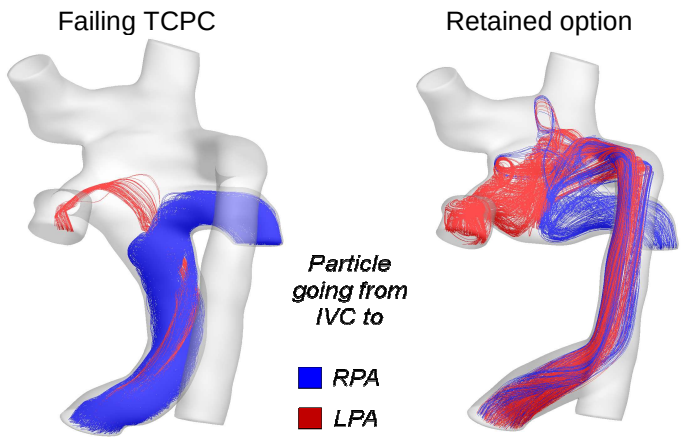

Figure 1-12: Hepatic flow distribution in the original failing TCPC and in the option retained for re-operation (CFD simulations)

Numerical (CFD) Exercise Studies on Patient Specific Anatomies (Published in Circulation[26] dx.doi.org/10.1161/CIRCULATIONAHA.106.680827): Physiological exercise simulations were performed on Fontan anatomies. The patients retained for the study were chosen from those who had already been enrolled in the Fontan project according to the following criteria: (i) availability of a 3D reconstruction, (ii) availability of an adequate metabolic exercise stress test to determine the maximum VO2, the VO2 at anaerobic threshold, the maximal work rate, and the oxygen pulse, (iii) and a maximum respiratory quotient of 1.2. From the current database, 13 patients were identified who met these criteria. The baseline resting flow rates and flow splits were obtained from PC MRI. Mild and intense exercise conditions were simulated as 2 and 3 times the baseline cardiac output, respectively. The entire increase in cardiac output was assumed to come from the IVC as is typically the case for lower limb exercises. The RPA/LPA flow splits during exercise were assumed to remain the same as under resting conditions. The relationship between cardiac output and power loss was found to be non-linear, with as much as a 45 fold increase in power loss from baseline to simulated maximal exercise. This may indicate that Fontan connections that have minimally different power losses at baseline may have significantly different losses at the increased flow rates of exercise. Furthermore, the preliminary data suggest that the power loss at baseline does not necessarily predict the power loss at exercise. TCPC efficiency should thus not only be characterized at baseline flow conditions, but also at under exercise conditions. Seven of the patients also had adequate exercise studies to compare to the power loss data. Results showed a negative trend between percent predicted maximal VO_2 and the TCPC resistances computed from CFD. However, the trend was not statistically significant and more data is needed to determine whether this trend will attain statistical significance. In addition to increasing the number of patients studied, attention will be placed on refining the model. In the current analysis, pulmonary flow splits are kept the same during exercise as at rest, which may not always be the case, especially in cases of significant PA stenosis. MRI imaging of Fontan patients during exercise in order to determine the effect of exercise on Fontan flows and on pulmonary flow splits should help us better refine our computational model.

Lumped Parameter Modeling to Represent Entire Circulation (Published in ASAIO[21] and AJP[43] dx.doi.org/ 10.1152/ajpheart.00628.2008): Lumped parameter models have been widely employed to investigate the function of the whole cardiovascular system. This approach exploits an analogy between fluid flow and electric circuits where pressure and flow rate would be analogous to voltage and current and models organs by their global hemodynamic status rather than anatomic configuration. The behavior of vascular trees is represented by a combination of resistors, inductors and capacitors to represent the viscous and inertial properties of blood, and the elastic wall behavior[44, 45]. The contraction of the heart is modeled using time-varying capacitors. Through a collaboration with the University of North Carolina, our group has developed and implemented a lumped parameter model of the singe ventricle circulation using MATLAB's Simulink. Although

conceptually straightforward, the parameters in the model do not necessarily have physiologic significance in that they cannot be directly measured. Instead, model parameters must be fit to pressure and flow data: 8 pressures (LV, AO, SVC, IVC, LA, RA, MPA, and respiratory) and 6 flows (AO, SVC, IVC, MPA, LPA, respiratory). After fitting these parameters, values can be modified throughout the lumped parameter model, mimicking the impact of an increased TCPC resistance, changes in systemic resistances and compliance, etc. Preliminary studies used this lumped-parameter model in combination with CFD results to investigate the potential benefit of coupling a pediatric ventricular assist device to the Fontan circulation[21] or estimate the impact of TCPC resistance upon the exercise capacity of the patient[43, 46]. TCPC resistance was estimated via CFD and then used in the lumped–parameter model. Results showed that cardiac output in Fontan patients strongly depended on vascular resistance. Figure 1-13A shows that for the average PVR of 1.8 Wood Units (WU), a 0.5 L/min increase in cardiac output can be achieved for every 0.56 WU reduction in TCPC resistance. In contrast a similar decrease in net resistance for the normal circulation would only produce about 10 times smaller increase in cardiac output (i.e., 0.05 l/min). Furthermore, the exercise simulation results (Figure 1-13B) prove that single ventricle patients had a severely reduced increase in CO (20% to 30% increase in Fontan patients vs. 67% in normals, at 140 bpm) and that this reduction worsened with higher TCPC resistances.

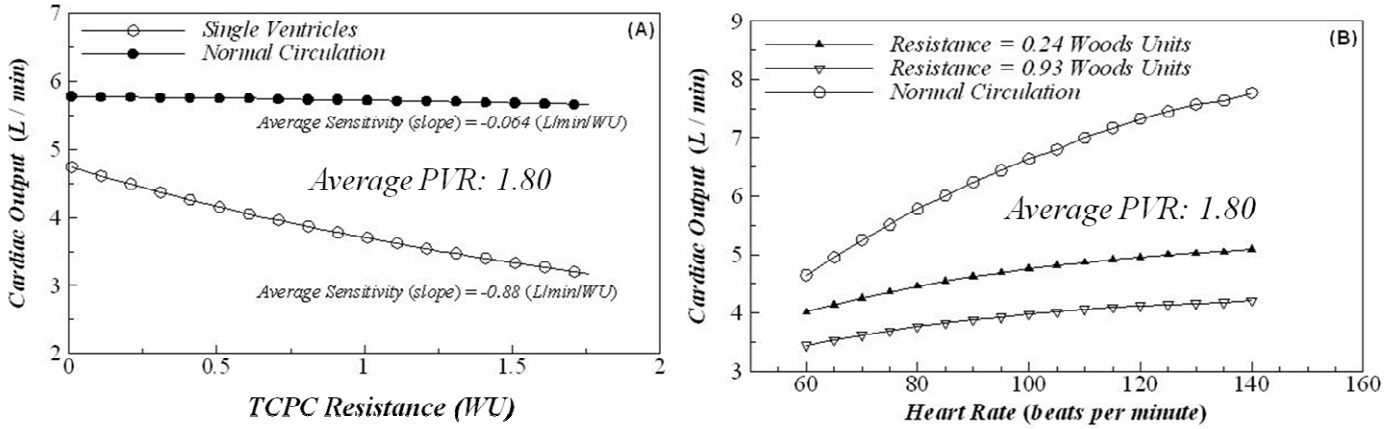

Figure 1-13: Impact of TCPC resistance in single ventricles vs. normal circulation, specifically resting cardiac output (A), and exercise cardiac output (B).

1.3. In vivo Lamb Studies (Published in JBME[47] and ABME[48], 3 submitted[49-51])

The main focus at UNC has been *in vivo* animal studies, where acute Fontan circulations were created in lambs to study the effects of geometry, graft material, and ventilation. These data were also used to generate a closed, lumped parameter model of the entire circulatory system and a preliminary structured tree representation of the pulmonary vasculature, which will allow for more accurate boundary conditions. Once the animals were euthanized, the Fontan connection was reserved for casting or *ex-vivo* studies. Finally, these animal studies also served for the investigation of novel TCPC procedures: Four types of Fontan procedures were investigated (Figure 1-14): atriopulmonary (AP) connections; an extra-cardiac TCPC where the IVC is directly implanted into the RPA (IVC-to-RPA); a classic extra-cardiac connection using an ePTFE (Gore, Flagstaff, AZ) graft (EC TCPC); and modified TCPC that implant the SVC into a Y-shaped ePTFE graft connecting the IVC and MPA (TCPY). Through the course of the BRP, **60 animal studies were attempted with post-operative data successfully collected for 24 studies**, distributed as follows: 11 AP, 4 IVC-to-RPA, 4 EC TCPC, and 5 TCPY.

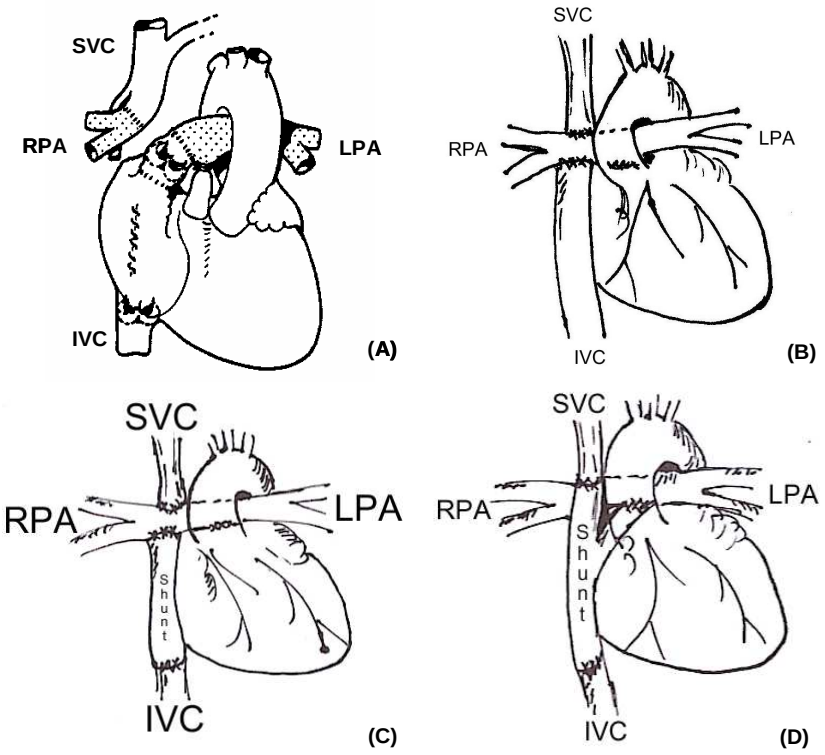

Figure 1-14: Investigated Fontan procedures: (A) AP connection, (B) TCPC, (C) TCPX, and (D) TCPY

1.3.1.1. Animal Study Protocol

Acute *in vivo* animal experiments were performed in lambs (10-20 kg) to closely approximate anatomy and physiology of children ranging from one month to three years old. Each animal was sedated using intramuscular ketamine, intubated, and ventilated with oxygen and isoflourane. Tidal volumes were adjusted to maintain optimal arterial blood gas tensions (approximately 10-15 mL/kg). Respiratory rate, CO_2 returns, and pulse oximetry (placed on the tongue) was monitored throughout the study. Prior to cardiopulmonary bypass, transducers were introduced into the region of interest. In the ventilation circuit, airflow was recorded using a Validyne pneumotachometer and airway pressure was recorded using a fluid filled polypropylene catheter inserted and connected to a Statham P23Gb transducer. To record vascular pressures, Millar™ MikroTip transducers were placed in the aorta (AOP), main pulmonary artery (MPA), superior vena cava (SVC), inferior vena cava (IVC,) right atrium (RA), left atrium (LA), left ventricle (LV). To record blood flow, Transonic™ T206 Small Animal Flow probes were positioned around the LPA, MPA, SVC, IVC, and aorta. Data was acquired using a custom LabVIEW interface at a rate of 200 Hz for episodes of 5.12 seconds. Control data were collected using the following respiratory protocol. While maintaining a constant respiratory rate of 13 breaths/min, stroke volume was varied in 100 cm^3 intervals from 200 to 700 cm^3/breath. Next, while maintaining a constant stroke volume of 400 cm^3, respiratory rate was varied in 5 breaths/min intervals from 8 to 23 breaths/min. Furthermore, keeping airflow rate constant at 5200 cm^3/min, combinations of respiratory rates and stroke volumes were performed. Multiple episodes of each parameter setting were recorded. Once control data was collected, pressure and flow transducers in the region of interest were removed. Cardiopulmonary bypass was performed using bi-caval and arterial cannulation at the aortic arch. Once on bypass, one of the Fontan modification procedures was performed. Pressure and flow transducers were repositioned and the respiratory protocol was repeated. Data analysis was performed using MATLAB.

1.3.1.1.1. Results

An overall summary of the measured hemodynamic parameters is shown in Table 1-3. The AP connection is fair, but has known physiologic consequences and is no longer used in practice. IVC-TO-RPA and TCPY offered the most favorable outcomes. A close examination of the data suggests that the IVC-TO-RPA had both the lowest systemic and pulmonary resistances and highest cardiac output. The TCPY exhibited a high-low

transition of cardiac output and systemic vascular resistance, suggesting that it favors higher ventilation. Finally, the EC TCPC, which used the same geometry as the IVC-TO-RPA but with a non-compliant shunt, showed the worst outcomes. Power loss was found to be lowest in the EC TCPC geometry, but this may be attributed to the low cardiac output.

Parameter	AP	IVC-to-RPA	EC TCPC	TCPY
CO (ml/s)	11.3	15.2	10.2	23
Transpulmonary gradient	11	10	22	6
PA pressure (mmHg)	17±3	20±6	29±4	27±9
IVC/SVC presure (mmHg)	19	25	25	22
Atrial pressure (mmHg)	16±6	10±5	7±3	21±13
PVR (Wood Unit) (Normal=7)	16	9	46	9
SVR (Wood Unit) (Normal=25)	38	37	57	26

Table 1-3: Measured hemodynamic parameters and changes relative to control

The time offset, or phase lag between pressure recorded in the pulmonary blood pressure and airway pressure was evaluated. The measured time offsets suggested that respiratory dynamics (i.e. diaphragm motion) also influenced the hemodynamics of the Fontan circulation. This may be observed from Figure 1-15 where we can see that, as expected, blood flow was independent of respiration (airway pressure), while blood pressure was modulated. It should be pointed out, however, that the exact nature of the modulation will depend on the breathing conditions (positive or negative ventilation, free breathing), so that these data acquired under positive ventilation should be used with care.

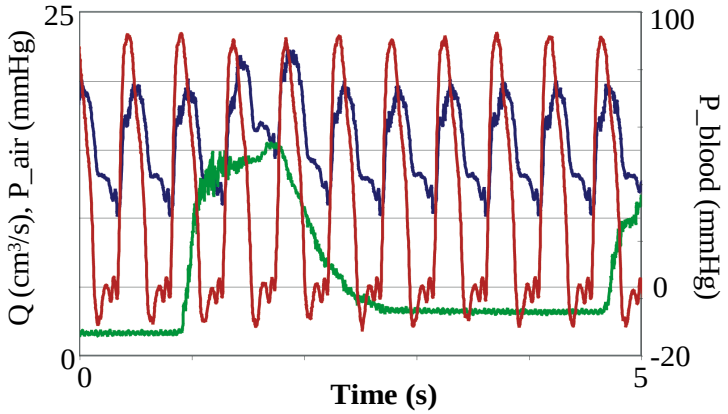

Figure 1-15: Animal data in the MPA: airway pressure (green), blood pressure (blue) and blood flow (red).

1.4. Development of an Anatomy Editing Tool for Surgical Planning Studies

1.4.1. Preliminary Surgical Planning Studies (Published in Circulation[32] and JTCVS[23])

Pioneering attempts towards patient-specific pre-surgical optimization were performed for two commonly encountered scenarios among the Fontan patients (Figure 1-16): (i) severe LPA stenosis due to aortic arch reconstruction and (ii) large IVC-to-LSVC offset in dual SVC cases. In these studies, patient anatomies were modified in the computer: For the first case, a virtual LPA angioplasty was performed, while, in the second case, the IVC was shifted towards the center of the connection, hoping for a better perfusion of the segment bounded by the two SVCs. Modified and original anatomies were run in CFD and their performances compared. For both cases, the virtual modifications brought in significant improvements in lung perfusion, cardiac output and cardiac energy loss, which are summarized in corresponding figure captions. **These**

studies were the first in a long line of detailed investigations, which will help in surgical decisions, and patients' clinical management and evaluation. However, for this process to be clinically feasible, the virtual surgery step should be user friendly, easy and fast. This requirement cannot be met with even the most advanced engineering CAD tools (Ideas, ProEngineer, Geomagics). To overcome these difficulties and come-up with a robust /practical surgical design tool for complex vascular anatomies a crucial collaboration has been established involving the PI, Dr. Ajit Yoganathan, and Dr. Jarek Rossignac of the College of Computing at GT.

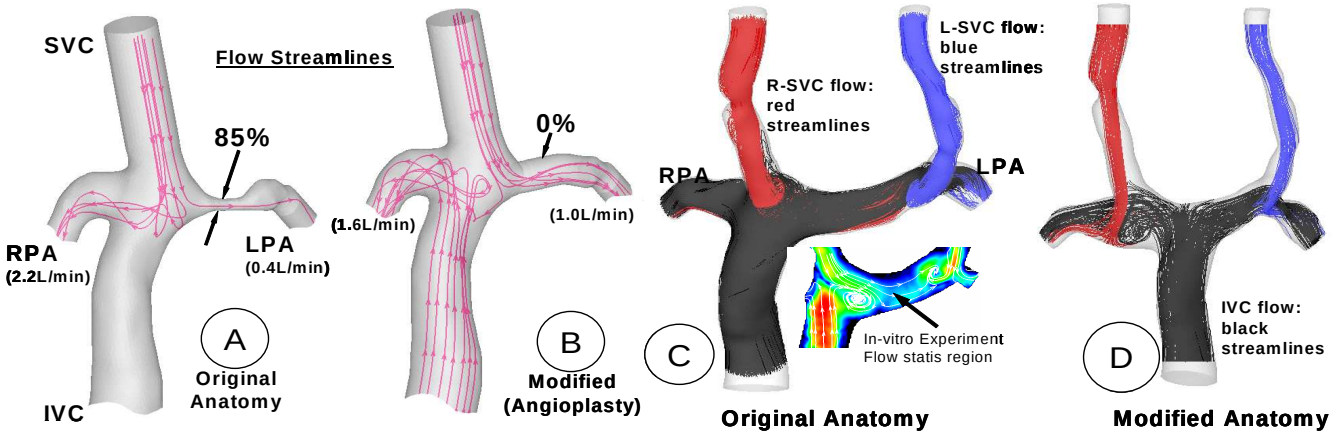

Figure 1-16: Virtual angioplasty (B) of an LPA stenosis (A). The modified anatomy resulted in 61% improvement in left lung perfusion and 50% reduction in hemodynamic power loss as compared to the modified anatomy[33]. No flow-stasis at the PA branch in between the two SVCs after relocating the IVC in the computer[24]. For the modified anatomy 11% increase in cardiac output is predicted due to 7% decrease in power loss.

1.4.2. Advanced Shape Modifying Tool: SURGEM® (Submitted to ABME[52])

Thanks to this collaboration, innovative robust geometrical morphing concepts (3D morphing, shape interaction, surface modification) were translated to the virtual surgical planning of single ventricle patients. The surgical planning tool, SURGEM® developed in the course of the original BRP builds upon Dr. Rossignac's early work in geometric modeling, graphics, 3D compression, Human-Shape interaction[53-56] and automatic 3D morphing[57, 58]. Once combined, these technologies allow the operator or surgeon to touch and manipulate a computer-controlled surface with bare hands, directly grabbing, pushing, pulling, and twisting it into the desired shape[59, 60]. Snapshots of the SURGEM® tool, the first generation anatomical editing/sculpturing hardware and software implementation are shown in Figure 1-17 as applied to the creation of a virtual extra-cardiac connection. The complete cardiovascular anatomic reconstruction of the single ventricle anatomy, including the BCPC, the heart, the aorta and the pulmonary veins, are imported into the tool. The red cylinder features the artificial graft to be implanted. Two haptic devices allow 3D anatomical orientation and interactive deformation of the anatomy in the computer with high efficiency and robustness, allowing the surgeon to place the graft as desired. As of now, the tool does not offer any stitching capability, and the final "virtual stitching" operation is accomplished offline using a commercial CAD package (Geomagic Studio 9.0 - Raindrop Geomagic, Research Triangle Park, N.C.). The resulting TCPC geometry may then be studied numerically or experimentally. During the initial development phase several brainstorming meetings were conducted with cardiologists and surgeons to identify the clinical scope of the proposed tool and employ their expertise to improve the tool. These inputs were carefully documented and used to prioritize the technology developments included in the subsequent BRP proposal.

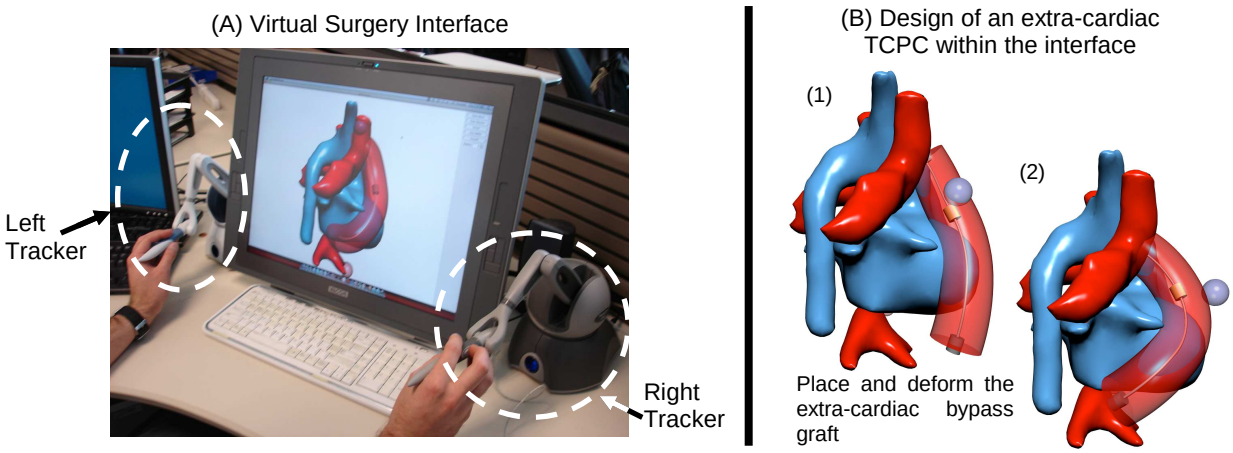

Figure 1-17: Example of a virtual surgery application. Patient TCPC (shown in red) and surrounding anatomical structures, such as the heart and great vessels (shown in blue), have been reconstructed from MRI and loaded into the virtual-surgical interface. Using two haptic trackers, one in each hand, the user/surgeon may directly interact with the geometry, here placing and deforming an artificial graft to complete the TCPC.

1.4.3. Preliminary Surgical Planning Scenarios Using SURGEM®

1.4.3.1. Morphing the Lumen: Glenn-Stage Designs

The first preliminary version of Surgem® could handle only one anatomical structure at a time and allowed only lumen surface deformations like bending or pulling type alterations. However, even at such a basic stage, this system proved relevant to study "What if?" scenarios. For example applied, it was applied to the parametric study of Glenn and Hemi-Fontan connections using patient-specific BCPCs. Figure 1-18 shows the resulting set of modified Glenn and hemi-Fontans, which took less than 20 min to design.

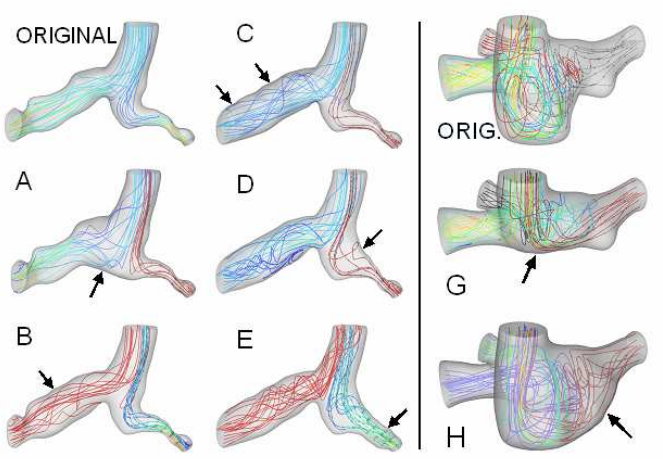

Figure 1-18: Original and free-deformed anatomical Glenn models (Left) and hemi-Fontans (Right). Anatomical modifications are pointed out by an arrow. The streamlines show the flow path in each model.

1.4.3.2. Surgical Planning of the 3rd Stage of the TCPC

Six patients, who were awaiting the final stage of the TCPC procedure, were retained from our anatomical MRI database. Five pediatric cardiac surgeons (Drs. Kirk Kanter and Paul Kirshbaum - Emory, Dr. Pedro del Nido – BCH, and Dr. William Gaynor - CHOP) were provided with the anatomical reconstruction of the Glenn stage anatomy as well as with a coronal MRI to roughly locate the neighboring organs. In this first study period, the human interaction system was only available at GT. Accordingly the surgeons sketched how they would construct the IVC baffle and a set of bioengineers at GT converted them into 3D digital models using

Surgem®, Figure 1-19. It is interesting to note that not all surgeons designed the connections the same way. For the patients who had already undergone the surgery, post-operative scans were available, that allowed the comparison between what was envisioned and what was actually done. This study and associated discussions with the surgeons may help us understand the reason behind the different surgical options. Finally, Surgem® allows for the generation of systematic TCPC variations (Figure 1-20). Even though the process is not automated yet and requires a few manual interventions, this lays a critical technological landmark for the proposed surgical planning and optimization of the TCPC.

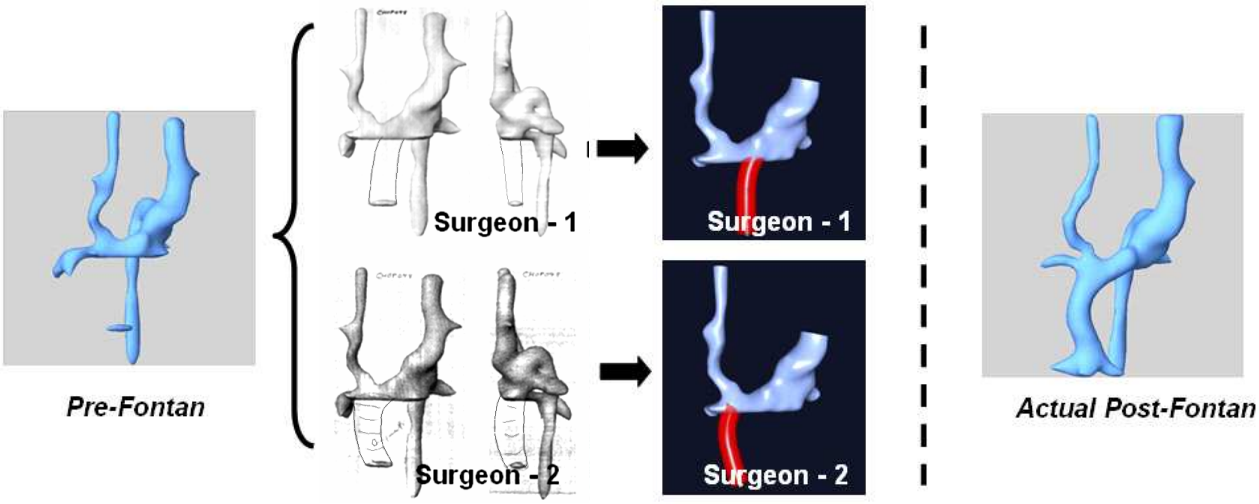

Figure 1-19: Given the 3D reconstruction of a pre-Fontan anatomy of different pediatric cardiac surgeons sketched their predicted Fontan anatomy. Right: actual post-Fontan anatomy

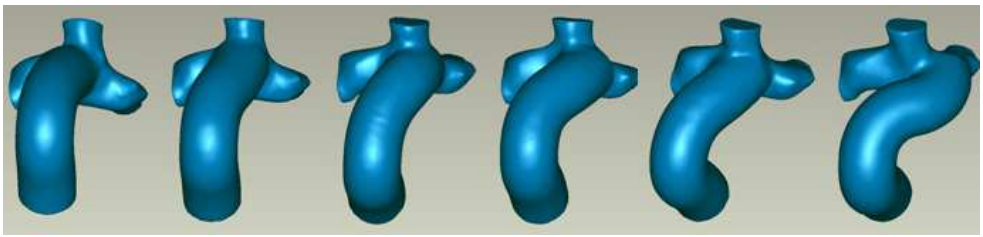

Figure 1-20: Extra-cardiac baffle variations

1.4.4. Pre-Operative Surgical Planning Applied in Clinical Setting

Combining the in vivo anatomy and flow analysis tools, SURGEM ® and our in house numerical solver, we have recently implemented our vision of the surgical planning into the clinical realm. These tools combined allow a) in depth analysis of the pre-operative hemodynamics and noninvasive quantification of the HFD to the lungs; and b) surgeons to virtually perform multiple surgical scenarios and determine the optimum one. This framework was applied for the pre-operative surgical planning of 5 patient cases, all of whom had pulmonary arteriovenous malformations (PAVMs). PAVMs are serious defects that are manifested in Fontan patients with abnormal hepatic flow distribution (HFD) to the lungs. Once the extent of PAVMs is such that oxygen saturation is critically low, the only palliative option is to re-operate and re-orient the hepatic baffle to achieve a better HFD[37]. Although several approaches for this palliative surgery have been proposed and discussed in the literature, there is still no consensus as to the best surgical approach to adopt for a specific patient. The small patient population and the large number of anatomical and functional variations pose a severe obstacle to the establishment of surgical guidelines from clinical studies alone. This is the typical clinical scenario where virtual surgical planning can make an impact.

The subsequent paragraphs summarize the experience gained over those 5 cases. All five patients were born with a complex heterotaxy syndrome and interrupted IVC, and were recommended for surgery because of severe PAVMs. Patients were separated into 2 groups: GpA (n=2) patients with persistent left superior vena cava (SVC) and GpB (n=3) patients with a single SVC. *In vivo* anatomies were reconstructed from MRI (4 pts) and CT (1 pt). Possible HB revisions (4 to 8 per pt) were generated using a virtual-surgery interface. HFD was assessed for all original connections and virtual revisions using a fully validated computational flow solver.
Figure 1-21 shows some of the options and associated performance obtained on three of these five patients. For patients with bilateral SVCs (GpA), ptimal results were obtained by connecting the hepatic baffle between the SVCs. Results were more individualized for patients with a single SVC (GpB). The best performing options including using a Y- shaped graft (1 pt) or a hepato-to-azygos shunt (2 pts). Under the pre-operative cardiac output distribution (COD), these optimized designs increased HFD to the diseased lung, which should in turn revert PAVM and rebalance COD, until equilibrium between HFD and COD is reached. On average, balanced HFD (50.9±10.1% HFD to the left) was predicted for an almost balanced COD (57.6±7.6% CO to the left lung).

Clinical follow up was available for one patient. Five month after the surgery, with the option identified during the surgical planning process, a clear improvement was reported in the overall clinical condition of the patient and oxygen saturation levels that had increased from 72 to 94%, implying regression of the PAVMs.

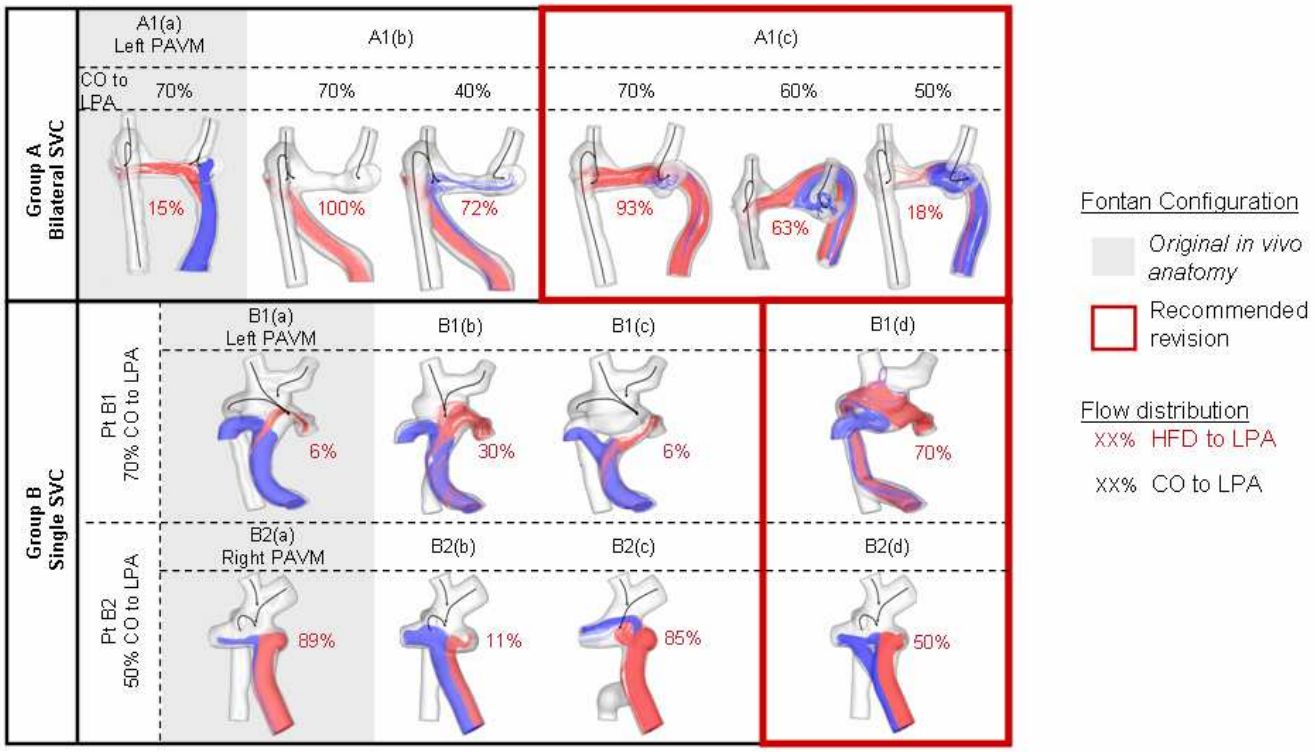

Figure 1-21: Surgical revisions for three patients (A1, B1 and B2). Percentages in red indicate hepatic flow going to the left lung. Superimposed black lines show the direction of the superior inflows. Connections shaded in gray show the in vivo configurations, others show possible revisions. Revisions highlighted in red point to the option recommended for surgery as these allowed hepatic flow split to adapt to the global cardiac output flow split. Establishment of the equilibrium between cardiac output and hepatic flow distributions is illustrated for patient A1, showing the hepatic flow distributions achieved over a wide range of for varying cardiac output distribution.

.

2. PUBLICATIONS

2.1. Published Books, Invited Book Chapters

1. Yoganathan, A.P., and Chatzimavroudis, G.P., "Hemodynamics," in Theory and Practice of Vascular Medicine". Lanzer, P, Topol, EJ, Eds. Springer-Verlag, 2002.
2. Yoganathan, A.P., and Kitajima, H., "Blood Flow – The Basics of the Discipline", pp. 38-54, Mark Fogel, Ed., Blackwell Futura, Malden, MA, 2005.
3. Lucas CL, Cole R, and Yoganathan A., "Closed Loop Modeling of Circulatory System", in Vascular Hemodynamics: Bioengineering and Clinical Perspectives. Editor: Peter Yim. John Wiley & Sons, Inc. Publication Date: April 2010.

2.2. Published Papers in Refereed Journals

1. Frakes, D., Conrad, C., Healy, T., Monaco, J., Smith, M., Fogel, M., Sharma, S., and Yoganathan, A.P., "Application of an Adaptive Control Grid Interpolation Technique to Morphological Vascular Reconstruction," IEEE Transactions on Biomedical Engineering, vol. 50, pp. 197-206, 2003.
2. Liu Y., Pekkan K., Jones C., Yoganathan A. P., "The Effects of Different Mesh Generation Methods on Fluid Dynamic Analysis and Power Loss in Total Cavopulmonary Connection (TCPC)," Journal of Biomechanical Engineering, Vol. 126, pp. 594-603, 2004.
3. Frakes, D., Pekkan, K., Smith, M.J.T., and Yoganathan, A. P., "Three-Dimensional Velocity Field Reconstruction," Journal of Biomechanical Engineering, Vol.126, pp.727-735, 2004.
4. Masters, J.C., Kettner, M., Mill, M., Yoganathan, A.P., and Lucas, C. L.,"The Effect of Incorporating Vessel Compliance in a Computational Model of Blood Flow ina Total Cavopulmonary Connection with Caval Centerline Offset," Journal of Biomechanical Engineering, Vol.126, pp.709-713, 2004.
5. de Zélicourt, D., Pekkan, K., Kitajima,K., Frakes,D., and A. P. Yoganathan., "Single-Step Stereolithography of Complex Anatomical Models for Optical Flow Measurements," Journal of Biomechanical Engineering, Vol. 127, pp. 205-207, 2005.
6. Pekkan, K., D. de Zélicourt, L. Ge, F. Sotiropoulos, D. H. Frakes, M. A. Fogel,and Yoganathan, A. P., "Physics-driven CFD modeling of complex anatomical cardiovascular flows-a TCPC case study," Annals of Biomedical Engineering, Vol.33, pp. 284-300, 2005.
7. Zelicourt D., Pekkan K., Wills L., Kanter K., Sharma S., Fogel M., Yoganathan A. P., "In Vitro Flow Analysis of a Patient Specific Intra-Atrial TCPC," Annals of Thoracic Surgery, Vol.79, pp. 2094-2102, 2005.
8. Pekkan K, Kitajima HD, de Zelicourt D, Forbess JM, Parks WJ, Fogel MA, Sharma S, Kanter KR, Frakes D, Yoganathan AP. Total cavopulmonary connection flow with functional left pulmonary artery stenosis: angioplasty and fenestration in vitro.Circulation, Vol. 112, pp: 3264-71, 2005.
9. Frakes D.H., Smith M.J.T., Parks J., Sharma S., Fogel M., Yoganathan A.P., "New Techniques for the Reconstruction of Complex Vascular Anatomies from MRI Images," Journal of Cardiovascular Magnetic Resonance, Vol. 7(2), pp: 425-432, 2005.
10. Pekkan K, Frakes D, de Zelicourt D, Lucas CW, Parks WJ, Yoganathan AP. Coupling Pediatric Ventricle Assist Devices to the Fontan Circulation: Simulations with a Lumped-Parameter Model. ASAIO J. Vol. 51, pp: 618-628, 2005.
11. de Zelicourt DA, Pekkan K, Parks J, Kanter K, Fogel M, Yoganathan AP.Flow study of an extra-cardiac connection with persistent left superior vena cava. Journal of Thoracic and Cardiovascular Surgery, Vol. 131, pp. 785-791, 2006.
12. Sudareswaran, K.S., Kanter, K.R., Kitajima, H.D., Krishnankutty, R., Sabatier, J., Parks, J., Sharma, S., Yoganathan, A.P., and Fogel, M.A., "Impaired Power Output and Cardiac Index with Hypoplastic Left Heart Syndrome – A Magnetic Resonance Imaging Study," Annals of Thoracic Surgery, Vol. 82, pp.167-77, 2006.
13. Whitehead, K. K., Pekkan, K., Kitajima, H.D., Paridon, S.M., Yoganathan, A.P., and Fogel, M.A. "Nonlinear Power Loss during Exercise in Single-Ventricle Patients after the Fontan: Insights From Computational Fluid Dynamics," Circulation, Vol. 116 (suppl.I), pp. I165-171, 2007.

14. Wang, C., Pekkan, K., deZélicourt, D., Horner, M., Parihar, A., Kulkarni, A., and Yoganathan, A.P., "Progress in the CFD Modeling of Flow Instabilities in Anatomical Total Cavopulmonary Connections," Annals of Biomedical Engineering, Vol. 36, pp. 1840-56, 2007.
15. Frakes, D., Pekkan, K., Dasi, L.P., Kitajima, H., Sundareswaran, K., Yoganathan, A.P., and Smith, M. "A New Adaptive Method of Registration-Based Medical Image Interpolation," IEEE Transactions on Medical Imaging, Vol. 27(3), pp. 370-7, 2008.
16. Kitajima H.D., Sundareswaran KS, Teisseyre TZ, Parks WJ, Skrinjar O, Oshinski JN, Yoganathan AP. "Comparison of Particle Image Velocimetry and Phase Contrast MRI of a Patient Specific Extra-Cardiac Total Cavopulmonary Connection," Journal of Biomechanical Engineering, Vol. 130(4), Article 041004, 2008.
17. Dasi L.P., Pekkan K., Katajima H.D., and Yoganathan A.P., "Functional Analysis of Fontan Energy Dissipation". Journal of Biomechanics, Vol. 41 (10), pp. 2246-2252, 2008.
18. Pekkan K., Dasi L.P., Nourparvar P., Yerneni S., Tobita K., Fogel M., Keller B., and Yoganathan A.P. "In Vitro Hemodynamic Investigation of Embryonic Aortic Arch at Late Gestation". Journal of Biomechanics, Vol 41 (8), pp. 1697-1706, 2008.
19. Krishnankutty R., Dasi L.P., Katajima H.D., Sundareswaran K.S., Pekkan K., Fogel M., Sharma S., Kanter K., and Yoganathan A.P. "Quantitative Analysis of Extracardiac Versus Intraatrial Fontan Anatomic Geometries". Annals of Thoracic Surgery, Vol. 85 (3), pp. 810-817, 2008.
20. Frakes D.H., Dasi L.P., Pekkan K., Katajima H., Yoganathan A.P., and Mark J.T. "A New Adaptive Method for Registration-Based Medical Image Interpolation". IEEE Transactions on Bio-Medical Engineering, Vol. 27 (3), pp. 370-377, 2008.
21. Pekkan K., Whited B., Kanter K., Sharma S., de Zelicourt D., Sundareswaran K., Frakes D., Rossignac J., and Yoganathan A.P. "Patient-Specific Surgical Planning and Hemodynamic Computational Fluid Dynamics Optimization through Free-Form Haptic Anatomy Editing Tool (SURGEM)". Medical Biology Engineering and Computing, Vol. 46(11), pp. 1139-52, 2008. Epub 2008 Aug 5.
22. Sundareswaran K.S., Pekkan K., Dasi L.P., Whitehead K., Sharma S., Kanter K.R., Fogel M.A., and Yoganathan A.P. "The Total Cavopulmonary Connection Resistance: A Significant Impact on Single Ventricle Hemodynamics at Rest and Exercise". American Journal of Physiology Heart and Circulatory Physiology, Vol. 295 (6), pp. H2427-H2435, 2009.
23. Sundareswaran K.S., Frakes D.H., Soerensen D.D.Fogel M.A., Oshinski J.N. Yoganathan A.P. "Optimum Fuzzy Filters for Phase Contrast MRI Segmentation." Journal of Magnetic Resonance Imaging, Vol. 29(1), pp. 155-165, 2009.
24. Dasi L.P., Krishnankutty R., Katajima H.D., Pekkan K., Fogel M., Sharma S., Kanter K., and Yoganathan A.P., "Fontan Hemodynamics: Importance of Pulmonary Artery Diameter". Journal of Thoracic and Cardiovascular Surgery, Vol. 137(3), pp. 560-564, 2009.
25. Pekkan K., Dasi L.P., de Zelicourt D.A., Sundareswaran K.S., Fogel M., Kanter K., and Yoganathan A.P. "Hemodynamic Performance of Stage-2 Univentricular Reconstruction: Glenn vs. Hemi-Fontan Templates". Annals of Biomedical Engineering, Vol. 37(1), pp. 50-63, 2009.
26. Dasi L.P., Pekkan K., de Zelicourt D.A., Sundareswaran K.S., Krishnankutty R., del Nido P.J., and Yoganathan A.P. "Hemodynamic Energy Dissipation in the Cardiovascular System: Generalized Theoretical Analysis on Disease States". Annals of Biomedical Engineering, Vol. 37(4), pp. 661-673, 2009.
27. Whitehead, K. K., Sundareswaran, K. S., Parks, J., Harris, M. A., Yoganathan, A. P., and Fogel, M. A. "Blood Flow Distribution in a Large Series of Fontan Patients: A Cardiac Magnetic Resonance Velocity Mapping Study". The Journal of Thoracic and Cardiovascular Surgery, Vol138(1), pp. 96-102, 2009.
28. de Zelicourt D., Ge L., Wang C., Sotiropoulos F., Gilmanov A., and Yoganathan A.P. "Flow Simulations in Arbitrarily Complex Cardiovascular Anatomies - an Unstructured Cartesian Grid Approach". Computers & Fluids, Volume 38(9), pp. 1749-62, 2009
29. Sundareswaran, K.S., de Zelicourt, D., Sharma, S., Kanter, K.R., Spray, T.L., Rossignac, J.R., Sotiropoulos, F., Fogel, M.A., and Yoganathan, A.P.; Correction of pulmonary artery arteriovenous malformations using image-based surgical planning; JACC imaging,Vol.2(8), pp. 1024-30, 2009.

2.3. Invited Conference, Lecture and Seminar Presentations

1. "Integrated Engineering Approach in the Assessment of Children Born with a Single Functioning Ventricle: The Total Cavopulmonary Connection," presented at Stanford University, CA, May 2002
2. "Fluid Dynamics of the Fontan Circulation", Plenary Lecture 10th International Congress on Biological and Medical Engineering, Singapore, December 2002.
3. "An Integrated Engineering Approach in the Assessment of Children Born with a Single Functioning Ventricle: The Total Cavopulmonary Connection," seminar presented at Virginia Polytechnique Institute and University, VA, April 2003.
4. "An Integrated Engineering Approach in the Assessment of Children Born with a Single Functioning Ventricle: The Total Cavopulmonary Connection," presented at Aarhus University, Denmark, October 2003
5. "An Integrated Approach in the Assessment of Children Born with a Single Functional Ventricle: The Total Cavopulmonary Connection," seminar given at the University of Colorado, Boulder, CO, April 2004.
6. "A Gallery of Cardiovascualar Flow Fields: From Heart Valves to Congenital Heart Disease," Key Note Lecture, 11th International Symposium on Flow Vizualization, Notre Dame University, IN, August 2004.
7. "Towards Understanding Anatomical Fluid Dynamics and Surgical Planning of the Total Cavo Pulmonary Connection, Grand Rounds, Cardiac Surgery and Cardiology," Boston Children's Hospital, Boston, MA, March 2005
8. "Surgical Planning of the Total Cavopulmonary Connection Using MR Imaging, Experimental and Computational Fluid Mechanics," Seminar, Deptartment of Biomedical Engineering, Yonsei University, S. Korea, October 2005
9. "Surgical Planning of the Total Cavopulmonary Connection Using MRI, Computational and Experimental Fluid Mechanics," Invited Talk, EMBE Conference, Prague, Czech Republic, November 2005
10. "Progress Towards Understanding the Fluid Dynamics Surgical Planning of the Total Cavopulmonary Connection," Invited Talk, 12th ICBME, Singapore, December 2005
11. "Surgical Planning of the Total Cavopulmonary Connection Using MRI, Computational and Experimental Fluid Mechanics" – Bioengineering seminar, California Institute of Technology, Pasadena, CA, January 2006
12. "Towards Understanding Anatomical Fluid Dynamics and Surgical Planning of the TCPC" – Bioengineering & Pediatric Cardiovascular Medicine seminar, University of Los Andes, Bogota, Colombia, April 2006
13. "Towards Understanding Anatomical Fluid Dynamics and Surgical Planning of the TCPC," Special Invited talk at Naming Ceremony of Department of Biomedical Engineering, University of Florida, Gainesville, FL, May 2006
14. "Towards Understanding Anatomical Fluid Dynamics and Surgical Planning of the TCPC," Pediatric Cardiology Grand Rounds, Children's Hospital of Philadelphia, PA, May 2006
15. "Towards Understanding Anatomical Fluid Dynamics and Surgical Planning of the TCPC," Surgery Grand Rounds, University of North Carolina, Chapel Hill, NC, June 2006
16. "Surgical Planning of the Total Cavopulmonary Connection Using MRI, Computational and Experimental Fluid Mechanics" – Biomedical Engineering and Cardiovascular Surgery seminar, University of Arhus, Denmark, June 2006
17. "Surgical Planning of the Total Cavopulmonary Connection Using MRI, Experimental and Computational Fluid Mechanics," Dept. of Bioengineering Seminar, University of Pittsburgh, PA, March 2007
18. "Surgical Planning of the Total Cavopulmonary Connection Using MRI, Experimental and Computational Fluid Mechanics," Dept. of Bioengineering Seminar, Penn State University, PA, March 2007
19. "Surgical Planning of the Total Cavopulmonary Connection Using MRI, Experimental and Computational Fluid Mechanics," Cardiac Surgery & Cardiology Seminar, Boston Children's Hospital, MA, May 2007.

20. "Surgical Planning of the Total Cavopulmonary Connection Using MRI, Experimental and Computational Fluid Mechanics," Dept. of Biomedical Engineering Seminar, Vanderbilt University, Nashville, TN, August 2007.
21. **"**Surgical Planning of the Total Cavopulmonary Connection Using MRI, Experimental and Computational Fluid Mechanics," Invited Keynote talk at Los Andes University Engineering Building Dedication, Bogota, Colombia, November 2007.
22. Yoganathan, A.P. "Computational Modeling and Image Libraries in Research", Pediatric Heart Network/NHLBI, Perioperative Working Group Meeting, Bethesda, April 6–7, 2009

2.4. Conference Presentations with Proceedings

1. Frakes, D., Smith, M., Fogel, M., Sharma, S., Yoganthan, A. Clinical Implementation of MR-Based Pediatric Cardiovascular Surgical Planning. Submitted to: Society for Cardiac Magnetic Resonance Annual Meeting, Orlando, Florida, February 2003.
2. Frakes, D., Sinotte, C., Conrad, C., Healy, T., Fogel, M., Monaco, J., Smith, M., Yoganathan, A. Application of an Adaptive Control Grid Interpolation Technique to MR Data Enhancement for Morphological Vascular Reconstruction. SPIE Medical Imaging Conference, San Diego, CA, February 2002.
3. Frakes, D., Lucas, C., Ensley, E., Healy, T., Sharma, S., and Yoganathan, A. Analysis of Total Cavopulmonary Connection Fluid Dynamics: Experimental Studies. 4th World Congress on Biomechanics, Calgary, Alberta, Canada, August 2002.
4. Soerensen, D.D., Jimenez, J., Christensen, T.B.N., He, Z., He, S., Honeycutt, C., and Yoganathan, A.P. Configuration of the Mitral Valves Subvalvular Complex and its Effect on the Chordal Force Distribution. Second Joint EMBS-BMES Conference, Houston, TX, October 2002.
5. Yoganathan, A.P. Fluid Dynamics of the Fontan Circulation, Plenary Lecture 10th International Congress on Biological and Medical Engineering, Singapore, December 2002.
6. Frakes, D.H., Sinotte, C.M., Parks, J., Sharma, S. and Yoganathan, A.P. Three-Dimensional Flow Field Reconstruction from Phase Encoded MR Velocity Images. The American Society of Mechanical Engineers, Summer Bioengineering Meeting, Key Biscayne, FL, June 2003.
7. Liu, Y., Ryu, K., Frakes, D.H. and Yoganathan, A.P. Fluid Dynamic Analysis and Power Loss Assessment for Total Cavopulmonary Connection Using Different Meshing Methods. The American Society of Mechanical Engineers, Summer Bioengineering Meeting, Key Biscayne, FL, June 2003.
8. Frakes, D.H., Sinotte, C.M., Parks, J., Sharma, S. and Yoganathan, A.P. Three-Dimensional Flow Field Reconstruction from Phase Encoded MR Velocity Images. The American Society of Mechanical Engineers, Summer Bioengineering Meeting, Key Biscayne, Florida, June 2003.
9. Liu, Y., Pekkan K., Jones, C., and Yoganathan, A.P. The Effects of Different Mesh Generation Methods on Fluid Dynamic Analysis and Power Loss in Total Cavopulmonary Connection (TCPC). ASME Summer Bioengineering Conference, Key Biscayne, Florida, June 2003.
10. de Zélicourt, D.A., Frakes, D., Pekkan, K. and Yoganathan, A.P. Construction of morphologically accurate TCPC models for in vitro flow studies. First US National Symposium on Frontiers in Biomechanics, Nashville, Tennessee, October 2003.
11. Wallin, A.K., Frakes, D.H., Brummer, M., Yoganathan, A.P. and Chapman, A.B. Improvements in Validation Studies: Polyvinyl Alcohol (PVA) Phantoms and Magnetic Resonance Imaging. Biomedical Engineering Society, Annual Fall Meeting, Nashville, Tennessee, October 2003.
12. Sorensen, D.D., Frakes, D.H., and Yoganathan, A.P. Automated Tracking of Heart Valve Leaflet Markers for Nonrigid Surface Motion Reconstruction. Biomedical Engineering Society, Annual Fall Meeting, Nashville, Tennessee, October 2003.
13. Pekkan, K., de Zélicourt, D. and Yoganathan, A.P. In vitro Visualization of an anatomic total cavopulmonary connection flow. 56th Annual Meeting APS division of fluid dynamics, East Rutherford, New Jersey, November 2003.
14. Frakes, D.H., Fogel, M.A., Parks, J., Sharma, S., Smith, M.J.T. and Yoganathan, A.P. MRI-Based 3D Modeling of Cardiac Vascular Anatomies for Surgical Applications. The American College of Cardiology Annual Scientific Session, New Orleans, LA, March 2004.

15. de Julien de Zélicourt, D.A, Pekkan K., Frakes, D. H., Carberry, J., Fogel, M. and Yoganathan, A. P. Fluid Mechanical Assessment of Anatomical Models of the Total Cavopulmonary Connection. 14th European Society of Bioengineering 2004, 's Hertogenbosch, The Netherlands, July 2004.
16. Pekkan, K., Kitajima, H., Forbess, J.M., Fogel, M., Kanter, K.R., Parks, J., Sharma, S., and Yoganthan, A.P. Total Cavopulmonary Connection Flow with Left Pulmonary Artery Stenosis. 14th European Society of Biomechanics Conference, Hertogenbosch,The Netherlands, July 2004.
17. Yoganathan, A.P., Frakes, D., Kitajima, H., Soerensen, D., Sundareswaran, K., Pekkan, K., Sotiropolous, F., deZelicourt, D. Flow Dynamics of the Anatomic TCPC: An Integrated MRI, In Vitro Experimentation, and CFD Approach for Surgical Applications. International Interdisciplinary Workshop on Flow and Motion, ISMRM, University Hospital Zurich, July 2004.
18. Soerensen, D.D., Pekkan, K., Sundareswaran, K.S., and Yoganathan, A.P. New Power Loss Optimized Fontan Connection Evaluated by Calculation of Power Loss Using High Resolution PC-MRI and CFD. 26th Annual International Conference of the IEEE Engineering in Medicine and Biology Society, San Francisco, CA, September, 2004.
19. Pekkan, K., Yoganathan, A.P., Frakes, D., Kitajima, H., Soerensen, D., Sundareswaran, K. and de Zelicourt, D. Progress towards understanding anatomical fluid dynamics and surgical planning of the TCPC. BMES Annual Fall Meeting, Philadelphia, PA, October 2004.
20. Yernenei, S, Pekkan, K., Kitajima, H., Soerensen, D.D., de Zelicourt, D., Parks, W.J., Sallee, D., Sharma, S., Fogel, M.A., and Yoganathan, A.P. Compurtaional Fluid Dynamics Study of an Intra-Atrial and Extra-Cardiac Patient-Specific Total Cavopulmonary Connection. Biomedical Engineering Society, Annual Fall Meeting, Philadelphia, PA, October, 2004.
21. Steele, B.N, Lucas, C.N., Ketner, M.E., Mill, M.R., Sheridan, B., Lucas, W.J., and Yoganathan, A. P. Energy Losses Due to Graft Compliance Under Steady and Pulsatile Flow in the Extracardiac TCPC. Biomedical Engineering Society, Annual Fall Meeting, Philadelphia, PA, October 13-16, 2004.
22. Ketner, M.E., Lucas, C.N., Mill, M.R., Sheridan, B., Lucas W.J., and Yoganathan, A.P. Energy Hemodynamics, and Respiration Effects in Lambs with Various Fontan Circulations. Biomedical Engineering Society, Annual Fall Meeting, Philadelphia, PA, October 13-16, 2004.
23. Pekkan, K., Kitajima, H., Forbess, J.M., Fogel, M., Kanter, K.R., Parks, J., Sharma, S., and Yoganthan, A.P. Functional Left Pulmonary Artery Stenosis in Total Cavopulmonary Connection (TCPC): Assessing Improvements in Lung Perfusion and Cardiac Workload with Computer Aided Angioplasty. The American Heart Association (AHA) Scientific Sessions New Orleans, LA, November 2004.
24. Gilmanov, A., Ge, L., Wang, C., de Zelicourt, D. Pekkan, K., Sotiropolous, F., and Yoganathan, A.P. Numerical Simulations of Flow in Anatomically Realistic Total Cavopulmonary Connections. 57th Annual Meeting of the Division of Fluid Dynamics, APS, Seattle, WA, November 2004.
25. Gilmanov, A., Ge, L., Wang, C., de Zelicourt, D., Pekkan, K., Sotiropolous, F., and Yoganathan, A.P. Flows in a Bileaflet Mechanical Heart Valve at Near Peak Systole Reynolds Number, 57th Annual Meeting of the Division of Fluid Dynamics, APS, Seattle, WA, November 2004.
26. Frakes D.H., Wake A.K., Pekkan K., Oshinski J., Giddens D.P., Yoganathan A.P., “Reconstruction of 3D PCMRA Data Sets for Clinical Fluid Dynamic Analysis Applications” International Society of Magnetic Resonance in Medicine (ISMRI) 13th Scientific Meeting, Miami, Florida, May 2005.
27. Sundareswaran K.S., Kitajima H., Pekkan K., Soerensen D.D., Yerneni V., Parks W.J., Sallee D., Yoganathan A.P., “Flow field comparison in reverse engineered total cavopulmonary connection anatomic models: High Resolution PC MRI vs CFD” International Society of Magnetic Resonance in Medicine (ISMRM) 13th Scientific Meeting, Miami, Florida, May 2005.
28. Pekkan K., Frakes D., Zelicourt D., Lucas C. W., W. Parks J., Yoganathan A. P, “Coupling of pediatric ventricle assist devices to Fontan circulation, simulations with a lumped parameter model.” First International Conference on Pediatric Mechanical Circulatory Support Systems and Pediatric Cardiopulmonary Perfusion, Hershey, Pennsylvania, May 2005.
29. Kitajima H.D., Sundareswaran K.S., Astary G.W., Parks W.J., Sharma S., Sallee D., Kanter K.R., Forbess J.M., Oshinski J.N., Yoganathan, A.P. “Comparison of Phase Contrast MRI and Particle Image Velocimetry of the Total Cavopulmonary Connection.” The American Society of Mechanical Engineering Conference, Vail, CO, June 2005.
30. Pekkan K., Soerensen D., Parks W.J., Kitajima H., Salee D., Fogel M., Yoganathan A.P., “Pre-Fontan surgery computational fluid dynamic analysis of three Glenn stage anatomies, Effects of innominate

vein and upper-lobe RPA branch," The American Society of Mechanical Engineering Conference, Vail, CO, June 2005.
31. Kitajima H.D., Teisseyre T., Sundareswaran K., Pekkan K., Oshinski J., Skrinjar O., Yoganathan A.P., Advantage of Semi-Automation over Manual Registration Comparing PIV and In Vitro PC-MRI Velocimetry, BMES Annual Meeting, Baltimore, MD, September/October 2005.
32. Lucas C.N., Ketner M., Steele B., Mill M. R., Sheridan B., Lucas W. J., Pekkan K., Yoganathan A. P., Toward an Understanding of the effects of Graft Compliance in Fontan Repairs, BMES Annual Meeting, Baltimore, MD, September/October 2005.
33. Pekkan K., Dasi L.P., Wang C., Zelicourt D., Sotiropoulos F., and Yoganathan A.P., "Fluid flow and dissipation in intersecting counter-flow pipes. Meeting of The American Physical Society, Chicago, IL, November, 2005. Also to appear in Bulletin of American Physical Society, Vol. 50 (2005).
34. Wang C., Gilmanov A., Ge L., Sotiropoulos F., and Yoganathan, A.P., 2005, "The Hemodynamics of Total Cavo-Pulmonary Connection Anatomies", Meeting of The American Physical Society, Chicago, IL, November, 2005.
35. Yoganathan, A.P., "Surgical Planning of the Total Cavopulmonary Connection Using MRI, Computational and Experimental Fluid Mechanics," Invited Talk, EMBE Conference Prague, Czech Republic, November 2005.
36. Frakes D.H., Pekkan K., Dasi L.P., Binnion R., Smith M.J.T., Yoganathan A.P., A New Adaptive Method for Registration-Based Medical Image Interpolation, 12th International Conference on Biomedical Engineering, Singapore, December 2005.
37. Lucas C., Ketner M., Steele B., Mill M., Sheridan B., Lucas W., Pekkan K., Yoganathan A.P., Using Lumped-Parameter Modeling to Improve Understanding of the Effects of Graft Compliance and Respiration in Fontan Repairs. 12th International Conference on Biomedical Engineering, Singapore, December 2005.
38. Kanter K.R., Sundareswaran K.S., Kitajima H.D., Soerensen D.D., Parks W.J., Fogel M.A., Yoganathan A.P. Impaired power output and cardiac index with hypoplastic left heart syndrome: a cardiac magnetic resonance imaging study. The Society of Thoracic Surgeons annual scientific meeting, Chicago, January-February 2006.
39. Kitajima H.D., Sundareswaran K.S., Teisseyre T.Z., Skrinjar O., Oshinski O.N., Yoganathan A.P. Phase contrast MRI velocimetry of a stereolithographic total cavopulmonary connection at 1.5T and 3.0T. International Society of Magnetic Resonance in Medicine, Seattle, May 2006.
40. Rossignac J, Pekkan K, Whited B, Kanter K, Yoganathan A, Surgem: Next Generation CAD tools targeting anatomical complexity for patient-specific surgical planning, Proceedings of ASME-Bio2006 Summer Bioengineering Conference, Florida, June 21-25, 2006.
41. Sundareswaran K.S., Fogel M.A., Yoganathan A.P. In vivo reconstruction of complex flows in single ventricle patients using phase contrast magnetic resonance imaging. International Society of Magnetic Resonance in Medicine Flow and Motion workshop New York, July 2006.
42. Kitajima H.D., Sundareswaran K.S., Teisseyre T.Z. et al. In vitro 3D particle image velocimetry of an extra-cardiac total cavopulmonary connection. 5th World Conference of Biomechanics, Munich, August 2006.
43. de Zélicourt D., Pekkan K., Sundareswaran K., Kitajima H., Rossignac J., Parks J., Sharma S., Kanter K., Fogel M., Yoganathan A.P. Progress towards surgical planning of the total cavopulmonary connection, 5th World Conference of Biomechanics, Munich, Germany, August 2006 (invited talk).
44. de Zelicourt D., Wang C., Sotiropoulos F., Yoganathan A.P., Unstructured Cartesian Sharp-Interface Computational Method for Flow Simulations in Realistic Cardiovascular Anatomies, 5th World Conference of Biomechanics, Munich, Germany, August 2006.
45. Lucas C., Ketner M., Steele B., Mill M.R., Sheridan B., Lucas W.J, Pekkan K., Yoganathan A.P., Importance of respiration and graft compliance in Fontan circulations: Experimental and computational studies, 5th World Conference of Biomechanics, Munich, Germany, August 2006
46. Pekkan K, Sasmazel A, Sundareswaran K, Parks WJ, Kanter K, Lucas C, Fogel M, Yoganathan A "Respiratory Augmentation of Blood Flow in the Early Post-Op Fontan Circulation – Feasibility of Intra-Pulmonic Balloon Pumping and External Counterpulsation of Systemic Venous Return" 16th World Congress of the World Society of Cardio-Thoracic Surgeons, Ottawa, Canada, August 17-20, 2006.

47. de Zelicourt D., Sundareswaran K.S., Pekkan K. et al. Surgical planning of the total cavopulmonary connection using MRI, computational and experimental fluid dynamics. American International Conference on Medical and Biological Engineering, AIMS in BioDesign, Atlanta, September 2006
48. Rossignac. K., Pekkan, K., de Zelicourt, D., Whited, B., Kanter, K., Sharma, S., Yoganathan, A., New Tools for Interactive Patient-Specific Cardiovascular Surgical Planning, American International Conference on Medical and Biological Engineering, AIMS in BioDesign, Atlanta, September 2006
49. Pekkan, K, de Zelicourt, D, Sundareswaran, K, Jimenez, J., Lucas, C., Yoganathan, A., Preliminary design of cardiovascular devices using lumped parameter modeling, American International Conference on Medical and Biological Engineering, AIMS in BioDesign, Atlanta, September 2006.
50. Sundareswaran K.S., Kitajima H.D., Yoganathan A.P. A fully automated mesh generator for experimental total cavopulmonary flow analysis. Biomedical Engineering Society annual conference, Chicago, October 2006.
51. Whitehead KK, Pekkan K, Kitajima HD, Paridon SM, Fogel MA, Yoganathan AP. Non-linear power loss during exercise in single ventricle patients after the Fontan - insights from computational fluid dynamics. Presented at Annual Scientific Sessions of the American Heart Association, Chicago, November 12-14, 2006
52. Sundareswaran K.S., Fogel M.A., Pekkan K., Kitajima H.D., Parks W.J., Sharma S., Yoganathan A.P. Viscous dissipation power loss of the total cavopulmonary connection evaluated using phase contrast magnetic resonance imaging. American Heart Association annual scientific sessions, Chicago November 2006.
53. Pekkan K., Nourparvar P., Yerneni S., Dasi L., de Zelicourt D., Fogel M., Yoganathan A.P. On the flow through the normal fetal aortic arc at late gestation , APS Division of Fluid Dynamics 59th Annual Meeting (DFD06), Tampa, Florida, November 2006.
54. de Zelicourt D., Wang C., Kitajima H., Pekkan K., Yoganathan A.P., Sotiropoulos F. Unstructured Cartesian/Immersed Boundary Method for Flow Simulation in Complex 3D Geometries, APS Division of Fluid Dynamics 59th Annual Meeting (DFD06), Tampa, Florida, November 2006.
55. Whitehead KK, Pekkan K, Kitajima H, Paridon S, Fogel M, Yoganathan A, Power Loss Analysis of Total Cavopulmonary Connections under Simulated Exercise Conditions Using Computational Fluid Dynamic Analysis, The American Heart Association (AHA) Scientific Sessions Chicago, Illinois, November 12–15 2006.
56. L.P. Dasi, K. Pekkan, K. Whitehead, M. Fogel, and A.P. Yoganathan, “Hepatic venous blood flow distribution in the total cavopulmonary connection: patient-specific anatomical models,” Proceedings of the ASME Summer Bioengineering Conference, Keystone, Colorado June 2007.
57. Krishnankuttyrema, R., Dasi, L.P., Pekkan, K., Sundareswaran, K., Kitajima, H.D., Yoganathan, A.P., A Skeletalized Representation of the Total Cavo-Pulmonary Connection, ASME Summer Bioengineering Conference, Keystone, CO, June 20-24, 2007.
58. Sundareswaran KS,de Zelicourt D, Pekkan K, Jayaprakash G, Kim D, Whited B, Rossignac J, Fogel M, Kanter K, Yoganathan. Anatomically Realistic Patient-Specific Surgical Planning of Complex Congenital Heart Defects Using MRI and CFD. Proceedings of the IEEE Engineering in Medicine and Biology Society Conference August 2007.
59. Restrepo M., Yerneni V.,Kim K., de Zelicourt D.A., Dasi L.P., Yoganathan A.P., Experimental Investigation of 2nd Stage Fontan Options: Glenn vs. Hemi-Fontan Connection, BMES Annual Meeting, Los Angeles, CA, September 2007
60. Sundarewaran S., Pekkan K., Dasi L.P., Kitajima H.D., Whitehead K., Fogel M., and Yoganathan A.P., Impact of the Total Cavopulmonary Resistance on Cardiac Output: Single vs. Dual Ventricle Circulation, The American Heart Association (AHA) Scientific Sessions Orlando, Florida, November 4–7 2007.
61. Whitehead K.K, Pekkan K., Doddasomayajula R., Kitajima H.D., Sundareswaran, K.S., Paridon S.M., Yoganathan A.P., Fogel, M.A., Computational Model of Exercise Effects on Fontan Hemodynamics Demonstrates Favorable Energetics In Extracardiac Fontans When Compared to Lateral Tunnel, The American Heart Association (AHA) Scientific Sessions Orlando, Florida, November 4–7 2007.

62. Sundareswaran K.S., Frakes D.H. Yoganathan A.P. “Rule-based Fuzzy Vector Median Filtering for 3D PCMRI Segmentation”. Oral Presentation. SPIE Computational Imaging VI., San Jose, CA, January 31-February 3, 2008.
63. Sundareswaran K.S., Frakes D.H., Fogel M.A., Skrinjar O., Yoganathan A.P. “Four Dimensional Velocity Field Reconstruction using Adaptive Divergence Free Radial Basis Functions”. Oral Presentation. Society of Cardiovascular Magnetic Resonance Annual Scientific Sesssions, Los Angeles, CA, January 31-February 3, 2008.
64. de Zelicourt, D., Sundareswaran, K., Dasi, L.P., Spray, T.L., Fogel, M., and Yoganathan, A.P. “Image-Based Surgical planning of the Total Cavopulmonary Connection - a Case Study”. Fifth International Bio-Fluid Symposium and Workshop, Pasadena, CA, March 28-30, 2008.
65. Sundareswaran K.S., Frakes D.H., Fogel M.A., Skrinjar O., Yoganathan A.P. “Multi-dimensional Velocity Field Reconstruction using Sparsely Acquired PC MRI data”. E-Poster. 16th Annual Meeting of International Society of Magnetic Resonance in Medicine, Toronto, Canada, May 4-8, 2008.
66. de Zelicourt D., Sundareswaran K., Whited B., Pekkan K., Dasi L.P., Rossignac J.R., Sotiropoulos F., and Yoganathan A.P. “Progress Towards Surgical Planning of the Total Cavopulmonary Connection”. Inaugural International Conference of the Engineering Mechanics Institute (EM08), Minneapolis, MN, May 18-21, 2008.
67. Sundareswaran K.S., de Zelicourt D.D., Dasi L.P., Yoganathan A.P., Fogel M.A. “Wasted Energy and Right Ventricular Volumes in Patients after Tetralogy of Fallot Repair: A Key to Understanding Right Heart Function”. E-Poster. American Heart Association Scientific Sessions, New Orleans, LA, November 8-12, 2008.
68. Sundareswaran K.S., Frakes D.H., de Zelicourt D.D., Skrinjar O., Kanter K.R., Del Nido P.J., Powell A.J., Fogel M.A., and Yoganathan A.P. “Comparison of Power Losses, Hepatic Flow Splits, and Vortex Sizes in Different Fontan Types using Non-Invasive Phase Contrast Magnetic Resonance Imaging”. American Heart Association Scientific Sessions, New Orleans, LA, November 8-12, 2008.
69. de Zelicourt, D., Ge, L., Sotiropoulos, F., and Yoganathan, A.P. “Efficient Unstructured Cartesian/Immersed-Boundary Method with Local Mesh Refinement to Simulate Flows in Complex 3D Geometries”. 61st Annual Meeting of the APS Division of Fluid Dynamics, San Antonio, TX, November 23-25, 2008.
70. de Zelicourt, D., Sundareswaran, K.S., Frakes, D.H., Fogel, M.A., Skrinjar, O., and Yoganathan, A.P. “Multi-dimensional reconstruction of velocity fields using sparsely acquired phase-contrast magnetic resonance images” , FDA / NHLBI / NSF Workshop on Computer Methods for Cardiovascular Devices, Rockville, June 1-2, 2009
71. Haggerty,C., Dasi, L., Kanter, J., and Yoganathan, A.P. “Effect of Flow Pulsatility on 2nd Stage Fontan Hemodynamics: An In Vitro Investigation” 2009 Summer Bioengineering Conference, Lake Tahoe, June 17-21, 2009

NOMENCLATURE

ACSL – A Computer Simulation Language
Ao – Aorta
AP - Atriopulmonary
CHOA – Children's Healthcare of Atlanta
CHOP – Children's Hospital of Philadelphia
CO – Cardiac output
CV – Cardiovascular
IVC – Inferior vena cava
LPA – Left pulmonary artery
LA – Left atrium
LAO – Inductive component of the walls
LV – Left ventricle
MPA – Main pulmonary artery
MRI – Magnetic resonance imaging
PC-MRI – Phase contrast magnetic resonance imaging
PIV – Particle image velocimetry
PPV – Positive pressure ventilation
PVR – Pulmonary vascular resistance
RA – Right atrium
RSVC – Right superior vena cava
RWAO – Viscoelastic component of the walls
SVC – Superior vena cava
SVR – Systemic vascular resistance
TCP – Total cavopulmonary
TCPC – Total cavopulmonary connection
TCPX –
TCPY – Total cavopulmonary connection with Y-shaped graft

3. REFERENCES

1. Sundareswaran, K., de Zélicourt, D., Sharma, S., Kanter, K., Spray, T., Rossignac, J.R., Sotiropoulos, F., Fogel, M., and Yoganathan, A.P., *Correction of pulmonary arteriovenous malformation using image based surgical planning.* JACC Imaging, 2009(Under Review).
2. Frakes, D.H., Conrad, C.P., Healy, T.M., Monaco, J.W., Fogel, M., Sharma, S., Smith, M.J., and Yoganathan, A.P., *Application of an adaptive control grid interpolation technique to morphological vascular reconstruction.* IEEE Trans Biomed Eng, 2003. 50(2): p. 197-206.
3. Frakes, D.H., Smith, M.J., Parks, J., Sharma, S., Fogel, S.M., and Yoganathan, A.P., *New techniques for the reconstruction of complex vascular anatomies from MRI images.* J Cardiovasc Magn Reson, 2005. 7(2): p. 425-32.
4. Frakes, D.H., Dasi, L.P., Pekkan, K., Kitajima, H.D., Sundareswaran, K., Yoganathan, A.P., and Smith, M.J., *An new method for registration-based medical image interpolation.* IEEE Trans Medic Imag, 2007(Article in Press).
5. Frakes, D., Smith, M., de Zelicourt, D., Pekkan, K., and Yoganathan, A., *Three-dimensional velocity field reconstruction.* J Biomech Eng, 2004. 126(6): p. 727-35.
6. Sundareswaran, K.S., Frakes, D., Soerensen, D., Fogel, M.A., and Yoganathan, A.P., *3D Phase Contrast Magnetic Resonance Imaging Segmentation using Fuzzy Vector Median Filters.* Journal of Magnetic Resonance Imaging, 2007(Under Review).
7. Kozerke, S., Botnar, R., Oyre, S., Scheidegger, M.B., Pedersen, E.M., and Boesiger, P., *Automatic vessel segmentation using active contours in cine phase contrast flow measurements.* J Magn Reson Imaging, 1999. 10(1): p. 41-51.
8. Xu, C.Y. and Prince, J.L., *Snakes, shapes, and gradient vector flow.* IEEE Transactions on Image Processing, 1998. 7(3): p. 359-369.
9. Krishnankutty, R., Dasi, L.P., Kitajima, H., Sundareswaran, K., Pekkan, K., Fogel, M., Sharma, S., Parks, J., Kanter, K., and Yoganathan, A.P., *Quantitative analysis of extra cardiac vs. intra atrial fontan anatomic geometries.* Annals of Thorasic Surgery, 2007(Under Review).
10. Krishnankutty, R., Dasi, L.P., Kitajima, H., Sundareswaran, K., Pekkan, K., Fogel, M., Sharma, S., Parks, J., Kanter, K., and Yoganathan, A.P., *Quantitative geometric comparison between extra cardiac and intra atrial Fontan anatomies.* Annals of Thorasic Surgery, 2007(Under Review).
11. Yang, Y., Zhu, L., Haker, S., Tannenbaum, A.R., and Giddens, D.P., *Harmonic skeleton guided evaluation of stenoses in human coronary arteries.* Medical Image Computing and Computer-Assisted Intervention - Miccai 2005, Pt 1, 2005. 3749: p. 490-497.
12. Steele, B.N., Draney, M.T., Ku, J.P., and Taylor, C.A., *Internet-based system for simulation-based medical planning for cardiovascular disease.* IEEE Trans Inf Technol Biomed, 2003. 7(2): p. 123-9.
13. Paik, D.S., Beaulieu, C.F., Jeffrey, R.B., Rubin, G.D., and Napel, S., *Automated flight path planning for virtual endoscopy.* Medical Physics, 1998. 25(5): p. 629-637.
14. Choi, Y., Rubin, G.D., Pitlik, P.T., Paik, D.S., Napel, S., and Wexler, L., *Virtual angioscopy of the aorta: Early experience with coarctation and patent ductus arteriosus.* Radiology, 1998. 209P: p. 439-440.
15. Buckley, J.A., Shifrin, R.Y., Paik, D.S., and Rubin, G.D., *Automated volumetric quantification of blood vessels using MR angiography.* Radiology, 1998. 209P: p. 475-475.
16. Paik, D.S., Rubin, G.D., and Napel, S., *Automatic segmentation of aortic thrombus and flow channel in CT angiography: Method and evaluation.* Radiology, 1998. 209P: p. 400-400.
17. Rubin, G.D., Paik, D.S., Johnston, P.C., and Napel, S., *Measurement of the aorta and its branches with helical CT.* Radiology, 1998. 206(3): p. 823-829.
18. Whitehead, K.K., Sundareswaran, K.S., Krishnankutty, R.A., Parks, W.J., Sharma, S., Hyslop, W.B., Yoganathan, A.R., and Fogel, M.A., *Impact of fontan type on blood flow distribution in a large series of single ventricle patients - A cardiac magnetic resonance velocity mapping study.* J Thorac Cardiovasc Surg, 2007(Under Review).
19. Sundareswaran, K.S., Kanter, K.R., Kitajima, H.D., Krishnankutty, R., Sabatier, J.F., Parks, W.J., Sharma, S., Yoganathan, A.P., and Fogel, M., *Impaired power output and cardiac index with hypoplastic left heart syndrome: a magnetic resonance imaging study.* Ann Thorac Surg, 2006. 82(4): p. 1267-75; discussion 1275-7.

20. Kanter, K., Sundareswaran, K., Kitajima, H., Soerensen, D., Fogel, M., Parks, J.W., and Yoganathan, A.P. *Impaired Power Output and Cardiac Index with Hypoplastic Left Heart Syndrome - A Phase Contrast Cardiac Magnetic Resonance Imaging Study*. in *The Society of Thoracic Surgeons Annual Meeting*. 2006. Chicago.
21. Pekkan, K., Frakes, D., De Zelicourt, D., Lucas, C.W., Parks, W.J., and Yoganathan, A.P., *Coupling pediatric ventricle assist devices to the Fontan circulation: simulations with a lumped-parameter model.* Asaio J, 2005. 51(5): p. 618-28.
22. de Zélicourt, D., Pekkan, K., Wills, L., Kanter, K., Forbess, J., Sharma, S., Fogel, M., and Yoganathan, A.P., *In vitro flow analysis of a patient-specific intraatrial total cavopulmonary connection.* Ann Thorac Surg, 2005. 79(6): p. 2094-102.
23. de Zélicourt, D., Pekkan, K., Parks, W.J., Kanter, K., Fogel, M., and Yoganathan, A.P., *Flow study of an extracardiac connection with persistent left superior vena cava.* J Thorac Cardiovasc Surg, 2006. 131(4): p. 785-91.
24. de Zélicourt, D., *A mechanical fluid assessment of anatomical models of the otal cavopulmonary connection (TCPC)*, in *Biomedical Engineering*. 2004, Georgia Institute of Technology: Atlanta.
25. Ensley, A.E., *A fluid mechanic assessment of the total cavopulmonary connection*, in *Biomedical Engineering*. 2000, Georgia Institute of Technology: Atlanta.
26. Whitehead, K.K., Pekkan, K., Kitajima, H.D., Paridon, S.M., Fogel, M.A., and Yoganathan, A.P., *Non-linear power loss during exercise in single ventricle patients after the Fontan - Insights from computational fluid dynamics.* Circulation, 2006. 114(18): p. 391-391.
27. Pekkan, K., de Zelicourt, D., Ge, L., Sotiropoulos, F., Frakes, D., Fogel, M.A., and Yoganathan, A.P., *Physics-driven CFD modeling of complex anatomical cardiovascular flows-a TCPC case study.* Ann Biomed Eng, 2005. 33(3): p. 284-300.
28. Liu, Y., Pekkan, K., Jones, S.C., and Yoganathan, A.P., *The effects of different mesh generation methods on computational fluid dynamic analysis and power loss assessment in total cavopulmonary connection.* J Biomech Eng, 2004. 126(5): p. 594-603.
29. Wang, C., Pekkan, K., de Zelicourt, D., Horner, M., Parihar, A., Kulkarni, A., and Yoganathan, A.P., *Progress in the CFD Modeling of Flow Instabilities in Anatomical Total Cavopulmonary Connections.* Ann Biomed Eng, 2007.
30. de Zélicourt, D., Ge, L., Wang, C., Sotiropoulos, F., Gilmanov, A., and Yoganathan, A.P., *Flow Simulations in Arbitrarily Complex Cardiovascular Anatomies - an Unstructured Cartesian Grid Approach.* Computers & Fluids, 2009. 38(9): p. 1749-62.
31. Pekkan, K., Dasi, L.P., de Zélicourt, D., Sundareswaran, K.S., Fogel, M.A., and Yoganathan, A.P., *Hemodynamic performance of stage-2 univentricular reconstruction: Glenn vs. hemi-Fontan templates.* Ann Biomed Eng, 2007(Under Review).
32. Pekkan, K., Kitajima, H.D., de Zelicourt, D., Forbess, J.M., Parks, W.J., Fogel, M.A., Sharma, S., Kanter, K.R., Frakes, D., and Yoganathan, A.P., *Total cavopulmonary connection flow with functional left pulmonary artery stenosis: angioplasty and fenestration in vitro.* Circulation, 2005. 112(21): p. 3264-71.
33. Dasi, L.P., Pekkan, K., Katajima, H.D., and Yoganathan, A.P., *Functional analysis of Fontan energy dissipation.* J Biomech, 2008. 41(10): p. 2246-52.
34. KrishnankuttyRema, R., Dasi, L.P., Kitajima, H., Pekkan, K., Sundareswaran, K., Fogel, M., Sharma, S., Whitehead, K., Kanter, K., and Yoganathan, A., *Fontan hemodynamics: Importance of pulmonary artery diameter.* J Thorac Cardiovasc Surg, 2009(Accepted for publication).
35. Hosein, R.B.M., Clarke, A.J.B., McGuirk, S.P., Griselli, M., Stumper, O., De Giovanni, J.V., Barron, D.J., and Brawn, W.J. *Factors influencing early and late outcome following the Fontan procedure in the current era. The 'Two Commandments'?* 2007.
36. Brown, J.W., Ruzmetov, M., Vijay, P., Rodefeld, M.D., and Turrentine, M.W., *Pulmonary arteriovenous malformations in children after the Kawashima operation.* Ann Thorac Surg, 2005. 80(5): p. 1592-6.
37. Duncan, B.W. and Desai, S., *Pulmonary arteriovenous malformations after cavopulmonary anastomosis.* Ann Thorac Surg, 2003. 76(5): p. 1759-66.
38. Moore, J.W., Kirby, W.C., Madden, W.A., and Gaither, N.S., *Development of pulmonary arteriovenous malformations after modified Fontan operations.* J Thorac Cardiovasc Surg, 1989. 98(6): p. 1045-50.
39. Pandurangi, U.M., Shah, M.J., Murali, R., and Cherian, K.M., *Rapid onset of pulmonary arteriovenous malformations after cavopulmonary anastomosis.* Ann Thorac Surg, 1999. 68(1): p. 237-9.

40. Shinohara, T. and Yokoyama, T., *Pulmonary arteriovenous malformation in patients with total cavopulmonary shunt: what role does lack of hepatic venous blood flow to the lungs play?* Pediatr Cardiol, 2001. 22(4): p. 343-6.
41. Pike, N.A., Vricella, L.A., Feinstein, J.A., Black, M.D., and Reitz, B.A., *Regression of severe pulmonary arteriovenous malformations after Fontan revision and "hepatic factor" rerouting.* Ann Thorac Surg, 2004. 78(2): p. 697-9.
42. Atz, A.M., Cohen, M.S., Sleeper, L.A., McCrindle, B.W., Lu, M., Prakash, A., Breitbart, R.E., Williams, R.V., Sang, C.J., and Wernovsky, G., *Functional state of patients with heterotaxy syndrome following the Fontan operation.* Cardiol Young, 2007. 17 Suppl 2: p. 44-53.
43. Sundareswaran, K.S., Pekkan, K., Dasi, L.P., Whitehead, K., Sharma, S., Kanter, K.R., Fogel, M.A., and Yoganathan, A.P., *The total cavopulmonary connection resistance: a significant impact on single ventricle hemodynamics at rest and exercise.* Am J Physiol Heart Circ Physiol, 2008. 295(6): p. H2427-35.
44. Westerhof, N. and Noordergraaf, A., *Arterial viscoelasticity: a generalized model. Effect on input impedance and wave travel in the systematic tree.* J Biomech, 1970. 3(3): p. 357-79.
45. Westerhof, N., Bosman, F., De Vries, C.J., and Noordergraaf, A., *Analog studies of the human systemic arterial tree.* J Biomech, 1969. 2(2): p. 121-43.
46. Sundareswaran, K., Pekkan, K, Kitajima, H, Dasi, L, Whitehead, K, Fogel, M, Yoganathan,A, *Significant Impact of the Total Cavopulmonary Resistance on Cardiac Output and Exercise Performance in Single Ventricles.* Circulation, 2007. Proceedings of the American Heart Association Annual Scientific Sessions 2007.
47. Masters, J.C., Ketner, M., Bleiweis, M.S., Mill, M., Yoganathan, A., and Lucas, C.L., *The effect of incorporating vessel compliance in a computational model of blood flow in a total cavopulmonary connection (TCPC) with caval centerline offset.* J Biomech Eng, 2004. 126(6): p. 709-13.
48. Cole, R.T., Lucas, C.L., Cascio, W.E., and Johnson, T.A., *A LabVIEW model incorporating an open-loop arterial impedance and a closed-loop circulatory system.* Ann Biomed Eng, 2005. 33(11): p. 1555-73.
49. Ketner, M.E., Lucas, C.l., Mill, M.R., Sheridan, B., Lucas, W., Steele, B., and Yoganathan, A.P., *Introduction of a Novel Total Cavo-Pulmonary with Y-Shaped Graft Connection Implemented in Lambs. .* Journal of Thoracic and Cardiovascular Surgery., 2007(Under Review).
50. Ketner, M.E., Lucas, C.l., Mill, M.R., Sheridan, B., Lucas, W., Steele, B., and Yoganathan, A.P., *Energetics of Positive Pressure Ventilation in Lamb Fontan Circulations.* Annals of Biomedical Engineering., 2007(Under Review).
51. Ketner, M.E., Lucas, C.l., Mill, M.R., Sheridan, B., Lucas, W., Steele, B., and Yoganathan, A.P., *Comparison of Hemodynamics in Lamb Models of the Fontan.* Circulation Research., 2007(Under Review).
52. Pekkan, K., Whited, B., Kanter, K., Krishnankutty, R., Sundareswaran, K., Frakes, D., Rossignac, J., and Yoganathan, A.P., *Patient specific surgical planning and hemodynamic computational fluid dynamic optimization through free-form haptic anatomy editing tool (SURGEM).* Annals of Biomedical Engineering, 2007(Under Review).
53. Rossignac, J. and Novak, M., *Research issues in model-based visualization of complex data-sets.* IEEE Computer Graphics & Applications, 1994. 14(2): p. 83-85.
54. Rossignac, J., *Representing and visualizing complex continuous geometric models*, in *Scientific Visualization: Advances and Challenges* L. Rosenblum, Editor. 1994, Academic Press. p. 337-348.
55. Rossignac, J. and O'Connor, M., *SGC: A dimension-independent model for pointsets with internal structures and incomplete boundaries*, in *Geometric Modeling for Product Engineering*, North-Holland, Editor. 1989. p. 145-180.
56. Rossignac, J., *Through the cracks of the solid modeling milestone*, in *From Object Modeling to Advanced Visualization*, S. Coquillart, W. Strasser, and P. Stucki, Editors. 1994, Springer Verlag. p. 1-75.
57. Kaul, A. and Rossignac, J.R., *Solid-Interpolating Deformations: Construction and Animation of PIPs.* Computers & Graphics, 1992. 16(1): p. 107-115.
58. Rossignac, J. and Kaul, A., *AGRELs and BIPs: Metamorphosis as a Bezier curve in the space of polyhedra.* Computer Graphics Forum, 1994(3): p. C179-C184.
59. Llamas, I., Powell, A., Rossignac, J.R., and Shaw, C. *Twister: A space-warp operator for the two-handed editing of 3D shapes.* in *ACM SIGGRAPH*. 2003.
60. Gargus, J., Kim, B., Llmas, I., and Rossignac, J., *Finger sculpturing with digital clay*. 2002, GVU Tech.